Acta Mech 226, 2195–2224 (2015)
DOI 10.1007/s00707-015-1304-8

A. R. Barati · M. Jabbari

Two-dimensional piezothermoelastic analysis of a smart FGM hollow sphere

Received: 9 October 2014 / Revised: 9 December 2014 / Published online: 12 February 2015

Abstract A two-dimensional analytical piezothermoelastic solution for a functionally graded material (FGM) hollow sphere with integrated piezoelectric layers as a sensor and actuator subjected to non-axisymmetric loads is carried out. A feedback gain control algorithm is used for the active control of stress and displacement of an FGM hollow sphere. The material properties of the FGM layer are assumed to be graded in the radial direction according to a power law function. Governing differential equations are developed in terms of the components of the displacement field, the electric potential, and the temperature of each layer of the smart FGM hollow sphere. These equations are solved analytically using the Legendre polynomials and the system of Euler differential equations. The effects of grading index of material properties and feedback gain on the mechanical–electrical responses are demonstrated in detail.

1 Introduction

The use of smart materials as sensors and actuators, for the control of the thermomechanical behavior of smart structural systems, is becoming more prevalent. Piezoelectric materials are one of the most common materials currently being investigated for smart structure applications due to their direct and converse piezoelectric effects, which allow them to be utilized as both actuators and sensors. The piezoelectric actuators make use of the direct effect of the piezoelectricity. In other words, they convert the input voltage into a strain/displacement actuation and then transmits this actuation to the main structure in order to modify its mechanical state. Consequently, an actuator has a good performance when we can get more stroke or strain for a specific voltage. The converse effect of the piezoelectricity is the principle that governs piezoelectric sensors. They convert a strain or displacement into an electrical field. In this case, a sensor possesses a good performance when it has high sensitivity to strain or displacement. There are two main fields to consider for piezoelectric sensors or actuators: the elastic and the electrical field. Moreover, thermal effects are present in almost all applications of smart structures and make enormous contributions as well. Sensing and controlling performance may change considerably when smart structures work in environments where temperature varies significantly. Many analytical studies concerning piezoelastic or piezothermoelastic problems have been reported, and their several books have been published [1]. A theoretical analysis of the control of displacement was developed for a composite rectangular plate constructed from an isotropic elastic layer and a piezoelectric layer due to non-uniform heat supply [2], and a piezothermoelastic plate [3,4] was obtained. In the case of spherical structures, Shul'ga [5] studied the radial electroelastic vibrations in a hollow piezoceramic sphere. By using the Frobenius series, an analytical solution for a non-homogeneous isotropic piezoelectric hollow sphere was created by Ding et al.

A. R. Barati (✉) · M. Jabbari
Mechanical Engineering Department, Islamic Azad University, South Tehran Branch, Tehran, Iran
E-mail: barati.ahmad@gmail.com
Tel.: +989126085863
Fax: +9866569613

[6]. Chen and Shioya [7] investigated the piezothermoelastic behavior of a pyroelectric spherical shell. Chen et al. [8] analytically investigated the problem of a piezoceramic hollow sphere based on the 3D equations of piezoelasticity. Dai and Wang [9] presented the stress wave propagation, and transient and dynamic responses in piezoelectric hollow spherical structures. By using the method of Laplace transformation, Ootao and Tanigawa [10] analyzed the transient piezothermoelastic problem for a functionally graded thermopiezoelectric hollow sphere based on the linear theory of thermoelasticity. Wang et al. [11] studied the dynamic problem of a multilayered piezoelectric sphere under spherically symmetric loading. The superposition method was used to divide the problem into quasi-static and dynamic parts. Wang and Xu [12] studied the effect of material inhomogeneity on the electromechanical behaviors of functionally graded piezoelectric spherical structures. Chen [13] analyzed three-dimensional free vibrations in a piezoceramic hollow sphere in which filled with a fluid; he considered three displacement functions for the mechanical displacement components in spherical coordinate and obtained the mechanical and thermal stresses, and the electrical potential, mechanical and electrical displacements along r, θ and $\emptyset$ using Bessel functions, and drew their graphs. Exact three-dimensional analysis for a linear piezoelectric hollow sphere was conducted by Chen [14]; he investigated the results for several pure material using three displacement function for displacement components and using Legendre polynomials. In [15], a three-dimensional analytical piezothermoelastic solution is presented for a functionally graded piezoelectric spherical shell subjected to various thermal boundary condition using the state space method. Furthermore, in [16], an exact solution is developed to obtain the mechanical and thermal stress and the electrical potential functions, the electrical and mechanical displacement in the two-dimensional steady-state (r, θ), a functionally graded piezoelectric porous material hollow sphere (FGPPM) by Jabbari et al.

The functionally graded materials (FGMs) are microscopically inhomogeneous material in which the mechanical properties vary smoothly and continuously from one surface to the other. They are used in modern technologies as advanced structures. It has many favorable performances in engineering application such as high resistance to large temperature gradient and reduction in stress concentration. The analytical solution for the one-dimensional steady-state thermomechanical stresses in a hollow thick sphere made of functionally graded material is given by Eslami et al. [17]. Obata and Noda [18] studied one-dimensional steady thermal stresses in a functionally graded circular hollow cylinder and a hollow sphere using the perturbation method. Jabbari et al. presented an analytical solution of one- and two-dimensional steady-state thermoelastic problems of the FGM cylinder [19,20]. A thick hollow sphere analysis using FGM under mechanical and thermal loads and in asymmetric and two-dimensional (r, θ) state was conducted investigating Navier equations and using Legendre polynomials [21]. With the increasing use of the smart material such as piezoelectrics, shape alloys, and rheological fluids, a smart functionally graded (FG) structural system with surface-bonded piezoelectric layers has attracted some researchers' attention. Noteworthy, analysis models on piezoelectric FG structures include those of Ootao and Tanigawa [22], and a 3D solution for rectangular FG plates coupled with a piezoelectric actuator layer was proposed by Reddy and Cheng [23] using transfer matrix and asymptotic expansion techniques. Wang and Noda [24] analyzed a smart FG composite structure composed of a layer of metal, a layer of piezoelectric, and an FG layer in between, while Huang and Shen [25] investigated the dynamics of an FG plate coupled with two monolithic piezoelectric layers at its top and bottom surfaces undergoing nonlinear vibrations in thermal environments. Reddy [26] presented the Navier solution and finite element models based on the classical and shear deformation plate theories for the analysis of laminated composite plates with integrated sensors and actuators, in which a simple negative velocity feedback control algorithm coupling the direct and converse piezoelectric effects was used to actively control an intelligent structure. Since this area is relatively new, very limited works can be found in the published literature for the active control of FGM structures using piezoelectric materials. Among those, Liew and his colleagues used classical laminated plate theory [27,28] and shallow shell model [29] to derive finite element formulation for the active piezothermoelastic control of FGM plates and shells, respectively. Thermomechanical instability of shallow spherical shells made of functionally graded material and surface-bonded piezoelectric actuators is studied in [30]. In the deflection control of PFGM beams, Ahmad et al. [31] developed an analytical solution for the analysis of functionally graded material beams containing two layers of piezoelectric material used as sensors and actuators. Xiao and Shen [32] studied the performance of the functionally graded plates integrated with the piezoelectric actuators. He et al. [33] examined the active control of a FGM plates with integrated piezoelectric sensor and actuators using the finite element method.

In this paper, an analytical study on the active control of a smart FGM hollow sphere with integrated piezoelectric sensor/actuator layers subjected to steady-state non-axisymmetric thermal loads is presented. The material properties of the FGM layer are assumed to be expressed by power functions in r. The feedback gain control algorithm is used in a closed control loop. Here, the output voltage of the sensor can be amplified

and is feedback to the actuator. Numerical examples are given and discussed to show the significant influence of grading index of material properties and negative feedback gain on the mechanical–electrical responses. This will be useful for modern engineering design.

2 Governing equations

This section outlines the foundations and steps required to develop the governing equations of a smart FGM hollow sphere. A spherical coordinate system (r, θ, ϕ) is adopted with the origin located at the center of the sphere. Figure 1 shows an FGM substrate hollow sphere with an inside radius a and an outside radius b that are integrated with the surface-bonded piezoelectric sensor (inner layer) and actuator (outer layer). Furthermore, in this smart structure, a_0 and b_0 are the inner and outer radius, respectively.

2.1 Piezoelectric layers

It is assumed that the electrical, mechanical, and thermal loads and their associated boundary conditions are such that the stress field is a function of variables r and θ. For the assumed condition, the strain–displacement relations in piezoelectric layers are

$$\varepsilon_{rr}^{a,s} = u_{,r}^{a,s}, \tag{1a}$$

$$\varepsilon_{\theta\theta}^{a,s} = \frac{u^{a,s}}{r} + \frac{1}{r} v_{,\theta}^{a,s}, \tag{1b}$$

$$\varepsilon_{\emptyset\emptyset}^{a,s} = \frac{u^{a,s}}{r} + \frac{v^{a,s}}{r} \cot\theta, \tag{1c}$$

$$\varepsilon_{r\theta}^{a,s} = \frac{1}{2}\left(\frac{1}{r} u_{,\theta}^{a,s} + v_{,r}^{a,s} - \frac{v^{a,s}}{r}\right), \tag{1d}$$

where $u^{a,s}$ and $v^{a,s}$ are the displacement components along the r and θ directions, respectively. Here, the suffixes "a" and "s" are used to denote the actuator and sensor layer, respectively.

The linear constitutive relations of a spherically isotropic piezoelectric medium are

$$\sigma_{rr}^{a,s} = c_{33}\varepsilon_{rr}^{a,s} + c_{13}\varepsilon_{\theta\theta}^{a,s} + c_{13}\varepsilon_{\emptyset\emptyset}^{a,s} + e_{22}E_r^{a,s} - z_r T^{a,s}(r,\theta), \tag{2a}$$

$$\sigma_{\theta\theta}^{a,s} = c_{11}\varepsilon_{\theta\theta}^{a,s} + c_{13}\varepsilon_{rr}^{a,s} + c_{12}\varepsilon_{\emptyset\emptyset}^{a,s} + e_{21}E_r^{a,s} - z_\theta T^{a,s}(r,\theta), \tag{2b}$$

$$\sigma_{\emptyset\emptyset}^{a,s} = c_{11}\varepsilon_{\emptyset\emptyset}^{a,s} + c_{13}\varepsilon_{rr}^{a,s} + c_{12}\varepsilon_{\theta\theta}^{a,s} + e_{21}E_r^{a,s} - z_\emptyset T^{a,s}(r,\theta), \tag{2c}$$

$$\sigma_{r\theta}^{a,s} = 2c_{44}\varepsilon_{r\theta}^{a,s} + e_{25}E_\theta^{a,s}, \quad \sigma_{\theta\emptyset}^{a,s} = \sigma_{r\emptyset}^{a,s} = 0, \tag{2d}$$

$$E_r^{a,s} = \frac{\partial\varphi^{a,s}}{\partial r}, \quad E_\theta^{a,s} = \frac{1}{r}\frac{\partial\varphi^{a,s}}{\partial\theta}, \tag{2e}$$

$$D_{rr}^{a,s} = e_{21}\varepsilon_{\theta\theta}^{a,s} + e_{21}\varepsilon_{\emptyset\emptyset}^{a,s} + e_{22}\varepsilon_{rr}^{a,s} - \varepsilon_{22}E_r^{a,s} + g_{22}T^{a,s}(r,\theta),$$

$$D_{\theta\theta}^{a,s} = 2e_{25}\varepsilon_{r\theta}^{a,s} - \varepsilon_{11}E_\theta^{a,s} + g_{21}T^{a,s}(r,\theta). \tag{2f}$$

Here, $\sigma_{ij}^{a,s}, \varepsilon_{ij}^{a,s}$ $(i, j = r, \theta, \emptyset)$, and $E_i^{a,s}$ $(i = r, \theta)$ are the stress and strain tensors and electrical field; $T^{a,s}(r,\theta)$ is the temperature distribution determined from the heat conduction equation; z_i and $g_{2i}(i = 1, 2)$ are the coefficients of thermal expansion in effective stress and pyroelectric constants; c_{ij}, e_{ij}, and ε_{ii} are the elastic, piezoelectric, and dielectric constants; $D_{ii}^{a,s}$ $(i = r, \theta)$ is the electrical displacement. Furthermore, we can have that

$$z_r = c_{33}\alpha_r + c_{13}\alpha_\theta + c_{13}\alpha_\emptyset = (c_{33} + 2c_{13})\alpha, \quad z_\theta = c_{11}\alpha_\theta + c_{13}\alpha_r + c_{12}\alpha_\emptyset = (c_{11} + c_{12} + c_{13})\alpha, \tag{3}$$

where α_i are the thermal expansion coefficients along the radial direction and along some direction perpendicular to the radial direction.

The equilibrium equations, disregarding the body forces and the inertia terms, are

$$\sigma_{rr,r} + \frac{1}{r}\sigma_{r\theta,\theta} + \frac{1}{r}(2\sigma_{rr} - \sigma_{\theta\theta} - \sigma_{\emptyset\emptyset} + \sigma_{r\theta}\cot\theta) = 0, \tag{4a}$$

$$\sigma_{r\theta,r} + \frac{1}{r}\sigma_{\theta\theta,\theta} + \frac{1}{2}((\sigma_{\theta\theta} - \sigma_{\emptyset\emptyset})\cot\theta + 3\sigma_{r\theta}) = 0. \tag{4b}$$

The charge equation of electrostatics is (in the absence of free charge density in the body)

$$\frac{1}{r^2}\frac{\partial}{\partial r}\left(r^2 D_{rr}\right)+\frac{1}{r\sin\theta}\frac{\partial}{\partial\theta}\left(D_{\theta\theta}\sin\theta\right)=0. \tag{5}$$

Employing a change in variable $\mu=\cos\theta$ and using Eqs. (1)–(5), the equilibrium equations in terms of the displacement components (Navier equations) are obtained as

$$\begin{aligned}
&u^{a,s}_{,rr}+\frac{2}{r}u^{a,s}_{,r}+\frac{2}{r^2}\left(\frac{c_{13}-c_{11}-c_{12}}{c_{33}}\right)u^{a,s}+\frac{1}{r^2}\frac{c_{44}}{c_{33}}\left(\left(1-\mu^2\right)u^{a,s}_{,\mu\mu}-2\mu u^{a,s}_{,\mu}\right)\\
&\quad+\frac{1}{r}\left(\frac{c_{13}+c_{44}}{c_{33}}\right)\left(-v^{a,s}_{,\mu}\sin\theta+v^{a,s}\cot\theta\right)_{,r}+\frac{1}{r^2}\left(\frac{c_{13}-c_{44}-c_{11}-c_{12}}{c_{33}}\right)\left(-v^{a,s}_{,\mu}\sin\theta+v^{a,s}\cot\theta\right)\\
&\quad+\frac{e_{22}}{c_{33}}\varphi^{a,s}_{,rr}+\frac{1}{2}\left(\frac{2\left(e_{22}-e_{21}\right)}{c_{33}}\right)\varphi^{a,s}_{,r}+\frac{1}{r^2}\frac{e_{25}}{c_{33}}\left(\left(1-\mu^2\right)\varphi^{a,s}_{,\mu\mu}-2\mu\varphi^{a,s}_{,\mu}\right)\\
&=\frac{z_r}{c_{33}}r^{-1}\left(\left(2-f\right)T^{a,s}+rT^{a,s}_{,r}\right),
\end{aligned} \tag{6a}$$

$$\begin{aligned}
&\left(v^{a,s}_{,rr}+\frac{2}{r}v^{a,s}_{,r}+\frac{1}{r^2}\frac{c_{11}}{c_{44}}\left(v^{a,s}_{,\theta\theta}+v^{a,s}\cot\theta\right)-\frac{1}{r^2}\left(2+\frac{c_{12}}{c_{44}}-\left(\frac{1}{1-\mu^2}-1\right)\frac{c_{11}}{c_{44}}\right)v^{a,s}-\frac{\left(1-\mu^2\right)}{r}\right)^{1/2}\\
&\quad\cdot\left(1+\frac{c_{13}}{c_{44}}\right)u^{a,s}_{,r\mu}-\frac{\left(1-\mu^2\right)^{\frac{1}{2}}}{r^2}\left(2+\frac{c_{11}+c_{12}}{c_{44}}\right)u^{a,s}_{,\mu}\left(\frac{\left(1-\mu^2\right)^{\frac{1}{2}}}{r^2}\right)\frac{2e_{25}}{c_{44}}\varphi^{a,s}_{,\mu}\\
&\quad-\frac{\left(1-\mu^2\right)^{1/2}}{r}\left(\frac{e_{25}+e_{21}}{c_{44}}\right)\varphi^{a,s}_{,r\mu}=-\frac{fz_r}{c_{44}}r^{-1}T^{a,s}_{,\mu}\left(1-\mu^2\right)^{\frac{1}{2}},
\end{aligned} \tag{6b}$$

$$\begin{aligned}
&u^{a,s}_{,rr}+\left(2+\frac{2e_{21}}{e_{22}}\right)\frac{1}{r}u^{a,s}_{,r}+\frac{2}{r^2}\frac{e_{21}}{e_{22}}u^{a,s}+\frac{1}{r^2}\frac{e_{25}}{e_{22}}\left(\left(1-\mu^2\right)u^{a,s}_{,\mu\mu}-2\mu u^{a,s}_{,\mu}\right)\\
&\quad+\frac{1}{2}\left(\frac{e_{21}+e_{25}}{e_{22}}\right)v^{a,s}_{,\mu}\sin\theta+\left(\frac{e_{21}+e_{25}}{e_{22}}\right)v^{a,s}_{,r}\cot\theta-\frac{1}{r^2}\left(\frac{e_{21}}{e_{22}}-\frac{e_{25}}{e_{22}}\right)\left(-v^{a,s}_{,\mu}\sin\theta+v^{a,s}\cot\theta\right)\\
&\quad-\frac{\varepsilon_{22}}{e_{22}}\varphi^{a,s}_{,rr}-\left(\frac{\varepsilon_{22}}{e_{22}}\right)\frac{2}{r}\varphi^{a,s}_{,r}-\frac{1}{r^2}\left(\frac{\varepsilon_{11}}{e_{22}}\right)\left(\left(1-\mu^2\right)\varphi^{a,s}_{,\mu\mu}-2\mu\varphi^{a,s}_{,\mu}\right)\\
&=-r^{-1}\left(\frac{g_{22}}{e_{22}}\right)\left(2T^{a,s}+rT^{a,s}_{,r}+S\left(-\left(1-\mu^2\right)^{\frac{1}{2}}T^{a,s}_{,\mu}+\frac{\mu}{\left(1-\mu^2\right)^{1/2}}T^{a,s}\right)\right),
\end{aligned} \tag{6c}$$

where

$$S=\frac{g_{21}}{g_{22}},\quad f=\frac{z_\theta}{z_r}. \tag{7}$$

2.2 FGM layer

The host layer's material is graded through the r-direction; thus, the material properties are functions of r. Let u^F and v^F be the displacement components along the r and θ directions, respectively. (the suffix "F" is used to denote the FGM layer). Then, the strain–displacement relations are

$$\varepsilon^F_{rr}=u^F_{,r}, \tag{8a}$$

$$\varepsilon^F_{\theta\theta}=\frac{u^F}{r}+\frac{1}{r}v^F_{,\theta}, \tag{8b}$$

$$\varepsilon^F_{\emptyset\emptyset}=\frac{u^F}{r}+\frac{v^F}{r}\cot\theta, \tag{8c}$$

$$\varepsilon^F_{r\theta}=\frac{1}{2}\left(\frac{1}{r}u^F_{,\theta}+v^F_{,r}-\frac{v^F}{r}\right). \tag{8d}$$

The two-dimensional stress–strain relations in the FGM hollow sphere are

$$\sigma_{rr}^{F} = \lambda e + 2\omega\varepsilon_{rr}^{F} - (3\lambda + 2\omega)\,\alpha T^{F}(r,\theta), \tag{9a}$$
$$\sigma_{\theta\theta}^{F} = \lambda e + 2\omega\varepsilon_{\theta\theta}^{F} - (3\lambda + 2\omega)\,\alpha T^{F}(r,\theta), \tag{9b}$$
$$\sigma_{\emptyset\emptyset}^{F} = \lambda e + 2\omega\varepsilon_{\phi\phi}^{F} - (3\lambda + 2\omega)\alpha T^{F}(r,\theta), \tag{9c}$$
$$\sigma_{r\theta}^{F} = 2\omega\varepsilon_{r\theta}^{F}, \quad \sigma_{\theta\emptyset}^{F} = \sigma_{r\emptyset}^{F} = 0, \tag{9d}$$

where σ_{ii} and ε_{ii} are the stress and strain tensors, $T^{F}(r,\theta)$ is the temperature distribution determined from the heat conduction equation, α is the coefficient of thermal expansion, and λ and μ are Lamé coefficients related to the modulus of elasticity E and Poisson's ratio ν as

$$\lambda = \frac{\nu E}{(1+\nu)(1-2\nu)}, \quad \omega = \frac{E}{2(1+\nu)}, \tag{10}$$
$$E(r) = E_0 r^{m_1}, \quad \alpha(r) = \alpha_0 r^{m_2}, \tag{11}$$

where E_0, α_0, m_1, and m_2 are the material constants. We may further assume that Poisson's ratio is constant.

Employing a change in variable $\mu = \cos\theta$ and using Eqs. (4) and (8)–(11), the equilibrium equations in terms of the displacement components (Navier equations) are obtained as

$$\begin{aligned} &u_{,rr}^{F} + \frac{(2+m_1)}{r}u_{,r}^{F} + \frac{2}{r^2}\left(\frac{\nu m_1}{1-\nu} - 1\right)u^{F} + \frac{1}{2r^2}\frac{1-2\nu}{1-\nu}\left(\left(1-\mu^2\right)u_{,\mu\mu}^{F} - 2\mu u_{,\mu}^{F}\right) \\ &\quad + \frac{1}{2r(1-\nu)}\left(-v_{,\mu}^{F}\sin\theta + v^{F}\cot\theta\right)_{,r} + \frac{1}{r^2}\left(\frac{\nu m_1}{1-\nu} - \frac{3-4\nu}{2-2\nu}\right)\left(-v_{,\mu}^{F}\sin\theta + v^{F}\cot\theta\right) \\ &\quad = \alpha_0 r^{m_2-1}\left((m_1+m_2)T^{F} + rT_{,r}^{F}\right)\frac{(1+\nu)}{(1-\nu)}, \end{aligned} \tag{12a}$$

$$\begin{aligned} &v_{,rr}^{F} + \frac{(2+m_1)}{r}v_{,r}^{F} + \frac{2}{r^2}\frac{1-\nu}{1-2\nu}\left(\left(1-\mu^2\right)v_{,\mu\mu}^{F} - 2\mu v_{,\mu}^{F}\right) \\ &\quad - \frac{1}{r^2}\left(m_1 + \frac{1}{1-\mu^2}\frac{2-2\nu}{1-2\nu}\right)v^{F} - \frac{(1-\mu^2)^{1/2}}{r(1-2\nu)}u_{,r\mu}^{F} - \frac{\left(1-\mu^2\right)^{\frac{1}{2}}}{r^2}\left(m_1 + \frac{4-4\nu}{1-2\nu}\right)u_{,\mu}^{F} \\ &\quad = -\alpha_0\frac{(1+\nu)}{(1-2\nu)}r^{m_2-1}T_{,\mu}^{F}\left(1-\mu^2\right)^{\frac{1}{2}}. \end{aligned} \tag{12b}$$

3 Heat conduction problems

The heat conduction equation in the steady-state condition for the two-dimensional problem in spherical coordinates is given as

$$T_{,rr} + \left(\frac{k'(r)}{k(r)} + \frac{2}{r}\right)T_{,r} + \frac{1}{r^2}\left(1-\mu^2\right)T_{,\mu\mu} - \frac{2}{r^2}\mu T_{,\mu} = 0, \quad -1 < \mu < 1. \tag{13}$$

where $k(r)$ is the thermal conduction coefficient that for the piezo and the FGM layers is, respectively,

$$k(r) = k_0 r^{m_3} \quad a < r < b, \quad k_0 \text{ is conduction coefficient (FGM layer)}, \tag{14a}$$
$$k(r) = k_p \quad a_0 < r < a, \quad \text{and} \quad b < r < b_0, k_p \text{ is conduction coefficient (piezoelectric layers)}. \tag{14b}$$

Substituting Eq. (14a) into Eq. (13) yields the FGM heat conduction equation as

$$T_{,rr}^{F} + \frac{1}{r}(m_3+2)\,T_{,r}^{F} + \frac{1}{r^2}\left(1-\mu^2\right)T_{,\mu\mu}^{F} - \frac{2}{r^2}\mu T_{,\mu}^{F} = 0. \tag{15}$$

Solution of the conduction equation may be assumed in the form of Legendre series as

$$T^{F}(r,\mu) = \sum_{n=0}^{\infty} T_n^{F}(r)P_n(\mu), \tag{16}$$

where $T_n^F(r)$ as the coefficient of Legendre series may be illustrated as

$$T_n^F(r) = \frac{2n+1}{2}\int_{-1}^{1} T^F(r,\mu)P_n(\mu)\mathrm{d}\mu = \frac{2n+1}{2}\int_0^{\pi} T^F(r,\theta)P_n(\cos\theta)\sin\theta\mathrm{d}\theta. \tag{17}$$

Using Eq. (16), Eq. (15) may be written as

$$\sum_{n=0}^{\infty}\left\{\left(\frac{\partial^2 T_n^F(r)}{\partial r^2}+\frac{1}{r}(m+2)\frac{\partial T_n^F(r)}{\partial r}\right)P_n(\mu)+\frac{1}{r^2}\left(\left(1-\mu^2\right)P_n''(\mu)-2\mu P_n'(\mu)\right)T_n^F(r)\right\}=0. \tag{18}$$

Employing the change in variable given in Appendix A results into the separation of independent variables in Eq. (18), which may be written as

$$\frac{\partial^2 T_n^F(r)}{\partial r^2}+\frac{1}{r}(m_3+2)\frac{\partial T_n^F(r)}{\partial r}-\frac{n^2+n}{r^2}T_n^F(r)=0. \tag{19}$$

The above equation is the Euler equation. Thus, the solution may be written in the form

$$T_n^F(r) = A_n^F r^{\beta^F}. \tag{20}$$

Substituting Eq. (20) into Eq. (19) yields

$$\beta_{n1,2}^F = \frac{-(m_3+1)\pm\sqrt{(m_3+1)^2+4n(n+1)}}{2}. \tag{21}$$

The general solution of Eq. (18) is

$$T_n^F(r) = A_{n1}^F r^{\beta_{n1}^F} + A_{n2}^F r^{\beta_{n2}^F}. \tag{22}$$

Thus, the temperature distribution becomes

$$T^F(r,\mu) = \sum_{n=0}^{\infty}\left(A_{n1}^F r^{\beta_{n1}^F} + A_{n2}^F r^{\beta_{n2}^F}\right)P_n(\mu). \tag{23}$$

Furthermore, for the piezoelectric layers by substituting Eq. (14b) into Eq. (13) and then with the similar solution process, the temperature distribution becomes

$$T^{a,s}(r,\mu) = \sum_{n=0}^{\infty}\left(A_{n1}^{a,s} r^{\beta_{n1}^{a,s}} + A_{n2}^{a,s} r^{\beta_{n2}^{a,s}}\right)P_n(\mu), \tag{24}$$

where

$$\beta_{n1,2}^{a,s} = \frac{-1\pm\sqrt{1+4n(n+1)}}{2}. \tag{25}$$

All the unknowns (A_{n1}^F, A_{n2}^F, $A_{n1}^{a,s}$, $A_{n2}^{a,s}$) can be evaluated by satisfying thermal boundary conditions

$$T^s(a_0,\theta) = T_1 P_n(\cos\theta), \qquad T^a(b_0,\theta) = T_2 P_n(\cos\theta), \tag{26}$$

and the continuity conditions on the interfaces

$$k_p\frac{\partial T^s}{\partial r} = k_0 r^{m_3}\frac{\partial T^F}{\partial r}, \qquad T^s(a,\theta) = T^F(a,\theta) \quad (r=a), \tag{27a}$$

$$k_0 r^{m_3}\frac{\partial T^F}{\partial r} = k_p\frac{\partial T^a}{\partial r}, \qquad T^F(b,\theta) = T^a(b,\theta) \quad (r=b). \tag{27b}$$

4 Analytical solution

4.1 Piezoelectric layers

The Navier equations (6a), (6b), and (6c) may be solved by a direct method of analysis employing the series solution that is assumed in the form of Legendre series as

$$u^{a,s}(r,\mu) = \sum_{n=0}^{\infty} u_n^{a,s}(r) P_n(\mu), \tag{28a}$$

$$v^{a,s}(r,\mu) = \sum_{n=0}^{\infty} v_n^{a,s}(r) P_n'(\mu)(1-\mu^2)^{1/2}, \tag{28b}$$

$$\varphi^{a,s}(r,\mu) = \sum_{n=0}^{\infty} \varphi_n^{a,s}(r) P_n(\mu), \tag{28c}$$

where $u_n^{a,s}(r)$, $v_n^{a,s}(r)$, and $\varphi_n^{a,s}(r)$ are functions of r. Substituting Eqs. (24) and (28) into Eqs. (6a), (6b), and (6c) and then using the method given in Appendix A to separate the independent variables r and μ lead to

$$\begin{aligned}
&\frac{\partial^2 u_n^{a,s}(r)}{\partial r^2} + \frac{2}{r}\frac{\partial u_n^{a,s}(r)}{\partial r} + \frac{1}{r^2}\left(-n(n+1)\frac{c_{44}}{c_{33}} + \frac{2c_{13} - 2(c_{11}+c_{12})}{c_{33}}\right) u_n^{a,s}(r) \\
&\quad + \frac{1}{r}\left(n(n+1)\left(\frac{c_{44}+c_{13}}{c_{33}}\right)\right)\frac{\partial v_n^{a,s}(r)}{\partial r} + \frac{n(n+1)}{r^2}\left(\frac{c_{13}-(c_{44}+c_{11}+c_{12})}{c_{33}}\right) v_n^{a,s}(r) \\
&\quad + \frac{e_{22}}{c_{33}}\frac{\partial^2 \varphi_n^{a,s}(r)}{\partial r^2} + \frac{1}{r}\left(\frac{2(e_{22}-e_{21})}{c_{33}}\right)\frac{\partial \varphi_n^{a,s}(r)}{\partial r} - \frac{n(n+1)}{r^2}\left(\frac{e_{25}}{c_{33}}\right)\varphi_n^{a,s}(r) \\
&= \frac{z_r}{c_{33}}\left((2-f)+\beta_{n1}^{a,s}\right) A_{n1}^{a,s}\, r^{\beta_{n1}^{a,s}-1} + \left((2-f)+\beta_{n2}^{a,s}\right) A_{n2}^{a,s}\, r^{\beta_{n2}^{a,s}-1},
\end{aligned} \tag{29a}$$

$$\begin{aligned}
&\frac{\partial^2 v_n^{a,s}(r)}{\partial r^2} + \frac{2}{r}\frac{\partial v_n^{a,s}(r)}{\partial r} - \frac{1}{r^2}\left(2 + n(n+1)\frac{c_{11}}{c_{44}} + \frac{c_{12}}{c_{44}}\right) v_n^{a,s}(r) \\
&\quad - \frac{1}{r}\left(1+\frac{c_{13}}{c_{44}}\right)\frac{\partial u_n^{a,s}(r)}{\partial r} - \frac{1}{r^2}\left(2+\frac{c_{11}+c_{12}}{c_{44}}\right) u_n^{a,s}(r) - \frac{2}{r^2}\frac{e_{25}}{c_{44}}\varphi_n^{a,s}(r) \\
&\quad - \frac{1}{r}\left(\frac{e_{25}+e_{21}}{c_{44}}\right)\frac{\partial \varphi_n^{a,s}(r)}{\partial r} = \frac{-f z_r}{c_{44}}\left(A_{n1}^{a,s}\, r^{\beta_{n1}^{a,s}-1} + A_{n2}^{a,s} r^{\beta_{n2}^{a,s}-1}\right),
\end{aligned} \tag{29b}$$

$$\begin{aligned}
&\frac{\partial^2 u_n^{a,s}(r)}{\partial r^2} + \frac{1}{r}\left(2+\frac{2e_{21}}{e_{22}}\right)\frac{\partial u_n^{a,s}(r)}{\partial r} + \frac{1}{r^2}\left(\frac{2e_{21}}{e_{22}} - n(n+1)\frac{e_{25}}{e_{22}}\right) u_n^{a,s}(r) \\
&\quad + \frac{n(n+1)}{2}\left(\frac{e_{21}+e_{25}}{e_{22}}\right)\frac{\partial v_n^{a,s}(r)}{\partial r} - \frac{n(n+1)}{r^2}\left(\frac{e_{21}-e_{25}}{e_{22}}\right) v_n^{a,s}(r) \\
&\quad - \left(\frac{\varepsilon_{22}}{e_{22}}\right)\frac{\partial^2 \varphi_n^{a,s}(r)}{\partial r^2} - \frac{2}{r}\left(\frac{\varepsilon_{22}}{e_{22}}\right)\frac{\partial \varphi_n^{a,s}(r)}{\partial r} + \frac{n(n+1)}{r^2}\left(\frac{\varepsilon_{11}}{e_{22}}\right)\varphi_n^{a,s}(r) \\
&= -\left(\frac{g_{22}}{e_{22}}\right)\left(2+Sn(n+1)+\beta_{n1}^{a,s}\right) A_{n1}^{a,s} r^{\beta_{n1}^{a,s}-1} + \left(2+Sn(n+1)+\beta_{n2}^{a,s}\right) A_{n2}^{a,s} r^{\beta_{n2}^{a,s}-1}.
\end{aligned} \tag{29c}$$

This is the system of Euler differential equations. Thus, the solution of the homogeneous part of Eqs. (29a), (29b), and (29c) may be assumed in the form

$$u_n^{a,s^g}(r) = B^{a,s} r^{\eta}, \tag{30a}$$

$$v_n^{a,s^g}(r) = C^{a,s} r^{\eta}, \tag{30b}$$

$$\varphi_n^{a,s^g}(r) = D^{a,s} r^{\eta}, \tag{30c}$$

where $B^{a,s}$, $C^{a,s}$, and $D^{a,s}$ are constants to be found using the given boundary conditions. Substituting Eqs. (30) into the homogeneous parts of Eqs. (29a), (29b), and (29c) yields

$$\begin{aligned}
&\left[\eta^2+2\eta+\left(-n\,(n+1)\,\frac{c_{44}}{c_{33}}+\frac{2c_{13}-2\,(c_{11}+c_{12})}{c_{33}}\right)\right]B^{a,s}\\
&+\left[n\,(n+1)\left(\frac{c_{44}+c_{13}}{c_{33}}\right)\eta+n\,(n+1)\left(\frac{c_{13}-(c_{44}+c_{11}+c_{12})}{c_{33}}\right)\right]C^{a,s}\\
&+\left[\left(\frac{e_{22}}{c_{33}}\right)\eta^2+\left(\frac{2\,(e_{22}-e_{21})}{c_{33}}-n\,(n+1)\,\frac{e_{25}}{c_{33}}\right)\right]D^{a,s}=0,
\end{aligned} \tag{31a}$$

$$\begin{aligned}
&\left[-\left(1+\frac{c_{13}}{c_{44}}\right)\eta-\left(2+\frac{c_{11}+c_{12}}{c_{44}}\right)\right]B^{a,s}+\left[\eta^2+2\eta-(2+n\,(n+1)\,\frac{c_{11}}{c_{44}}+\frac{c_{12}}{c_{44}})\right]C^{a,s}\\
&-\left[\left(\frac{e_{25}+e_{21}}{c_{44}}\right)\eta+\frac{2e_{25}}{c_{44}}\right]D^{a,s}=0,
\end{aligned} \tag{31b}$$

$$\begin{aligned}
&\left[\eta^2+\left(2+\frac{2e_{21}}{e_{22}}\right)\eta+\left(\frac{2e_{21}}{e_{22}}-n\,(n+1)\,\frac{e_{25}}{e_{22}}\right)\right]B^{a,s}+\left[n\,(n+1)\left(\left(\frac{e_{21}+e_{25}}{e_{22}}\right)\eta-\frac{e_{21}}{e_{22}}-\frac{e_{25}}{e_{22}}\right)\right]C^{a,s}\\
&-\left[\left(\frac{\varepsilon_{22}}{e_{22}}\right)\eta^2+\left(\frac{2\varepsilon_{22}}{e_{22}}\right)\eta-n\,(n+1)\left(\frac{\varepsilon_{11}}{e_{22}}\right)\right]D^{a,s}=0.
\end{aligned} \tag{31c}$$

To obtain the non-trivial solution of the above equation, the determinant of the coefficients of the constants $B^{a,s}$, $C^{a,s}$, and $D^{a,s}$ must vanish. This leads to the evaluation of the eigenvector η obtained as

$$\begin{aligned}
&\left(\eta^2+2\eta+\left(-n\,(n+1)\,\frac{c_{44}}{c_{33}}+\frac{2c_{13}-2\,(c_{11}+c_{12})}{c_{33}}\right)\right)\times\left(\eta^2+2\eta-(2+n\,(n+1)\,\frac{c_{11}}{c_{44}}+\frac{c_{12}}{c_{44}})\right)\\
&\times\left(\left(\frac{\varepsilon_{22}}{e_{22}}\right)\eta^2+\left(\frac{2\varepsilon_{22}}{e_{22}}\right)\eta-n\,(n+1)\left(\frac{\varepsilon_{11}}{e_{22}}\right)\right)-\left(\left(\frac{e_{25}+e_{21}}{c_{44}}\right)\eta+\frac{2e_{25}}{c_{44}}\right)\\
&\times\left(n\,(n+1)\left(\left(\frac{e_{21}+e_{25}}{e_{22}}\right)\eta-\frac{e_{21}}{e_{22}}-\frac{e_{25}}{e_{22}}\right)\right)\\
&-\left(n\,(n+1)\left(\frac{c_{44}+c_{13}}{c_{33}}\right)\eta+n\,(n+1)\left(\frac{c_{13}-(c_{44}+c_{11}+c_{12})}{c_{33}}\right)\right)\\
&\times\left(\eta^2+2\eta+\left(-n\,(n+1)\,\frac{c_{44}}{c_{33}}+\frac{2c_{13}-2\,(c_{11}+c_{12})}{c_{33}}\right)\right)\times\left(\left(\frac{\varepsilon_{22}}{e_{22}}\right)\eta^2+\left(\frac{2\varepsilon_{22}}{e_{22}}\right)\eta-n\,(n+1)\left(\frac{\varepsilon_{11}}{e_{22}}\right)\right)\\
&-\left(\left(\frac{e_{22}}{c_{33}}\right)\eta^2+\left(\frac{2\,(e_{22}-e_{21})}{c_{33}}-n\,(n+1)\,\frac{e_{25}}{c_{33}}\right)\right)\times\left(\eta^2+\left(2+\frac{2e_{21}}{e_{22}}\right)\eta+\left(\frac{2e_{21}}{e_{22}}-n\,(n+1)\,\frac{e_{25}}{e_{22}}\right)\right)\\
&+\left(\eta^2+\left(2+\frac{2e_{21}}{e_{22}}\right)\eta+\left(\frac{2e_{21}}{e_{22}}-n\,(n+1)\,\frac{e_{25}}{e_{22}}\right)\right)\\
&\times\left(\eta^2+2\eta+\left(-n\,(n+1)\,\frac{c_{44}}{c_{33}}+\frac{2c_{13}-2\,(c_{11}+c_{12})}{c_{33}}\right)\right)\times\left(\eta^2+2\eta-(2+n\,(n+1)\,\frac{c_{11}}{c_{44}}+\frac{c_{12}}{c_{44}})\right)\\
&\times\left(\left(\frac{\varepsilon_{22}}{e_{22}}\right)\eta^2+\left(\frac{2\varepsilon_{22}}{e_{22}}\right)\eta-n\,(n+1)\left(\frac{\varepsilon_{11}}{e_{22}}\right)\right)\\
&-\left(n\,(n+1)\left(\frac{c_{44}+c_{13}}{c_{33}}\right)\eta+n\,(n+1)\left(\frac{c_{13}-(c_{44}+c_{11}+c_{12})}{c_{33}}\right)\right)\\
&\times\left(-\left(1+\frac{c_{13}}{c_{44}}\right)\eta-\left(2+\frac{c_{11}+c_{12}}{c_{44}}\right)\right)=0.
\end{aligned} \tag{32}$$

Thus, the general solution, utilizing the linearity lemma, is a linear combination of all values of eigenvalues and is obtained as

$$u_n^{a,s^g}(r) = \sum_{j=1}^{6} B_{nj}^{a,s}\, r^{\eta_{nj}}, \quad v_n^{a,s^g}(r) = \sum_{j=1}^{6} N_{nj} B_{nj}^{a,s}\, r^{\eta_{nj}}, \quad \varphi_n^{a,s^g}(r) = \sum_{j=1}^{6} M_{nj} B_{nj}^{a,s} r^{\eta_{nj}}, \tag{33}$$

where using Eq. (31), M_{nj} and N_{nj} may be found as

$$\begin{aligned} M_{nj} = {} & \left(n\,(n+1)\,(c_{13}+c_{44})\,\eta_{nj} + n\,(n+1)\,(c_{13}-(c_{44}+c_{11}+c_{12}))\right) \\ & \cdot \left((c_{13}+c_{44})\,\eta_{nj} + (2c_{44}+c_{11}+c_{12})\right) / \left(2c_{44}+n\,(n+1)\,c_{11}+c_{12}\right) \\ & \times \left(e_{22}\eta_{nj}^2 + 2\,(e_{22}-e_{21}) - n\,(n+1)\,e_{25}\right) - \left(n\,(n+1)\,(c_{13}+c_{44})\,\eta_{nj} + n\,(n+1)\right)^{-1} \\ & - \frac{\left(2c_{44}+n\,(n+1)\,c_{11}+c_{12}\right)\left(c_{33}\eta_{nj}^2 + 2c_{33}\eta_{nj} - n\,(n+1)\,c_{44} + 2(c_{13}-(c_{11}+c_{12}))\right)}{c_{13}-(c_{44}+c_{11}+c_{12})\left((e_{21}+e_{25})\,\eta_{nj}+2e_{25}\right)}, \end{aligned} \tag{34a}$$

$$\begin{aligned} N_{nj} = {} & \frac{\left((e_{21}+e_{25})\,\eta_{nj}+2e_{25}\right)\left(c_{33}\eta_{nj}^2 + 2c_{33}\eta_{nj} - n\,(n+1)\,c_{44} + 2(c_{13}-(c_{11}+c_{12}))\right)}{\left(e_{22}\eta_{nj}^2 + 2\,(e_{22}-e_{21}) - n\,(n+1)\,e_{25}\right)\left(c_{44}\eta_{nj}^2 + 2c_{44}\eta_{nj} - (2c_{44}+n\,(n+1)\,c_{11}+c_{12})\right)} \\ & - \frac{\left(e_{22}\eta_{nj}^2 + 2\,(e_{22}-e_{21}) - n\,(n+1)\,e_{25}\right)\left((c_{13}+c_{44}) - (2c_{44}+c_{11}+c_{12})\right)}{\left((e_{21}+e_{25})\,\eta_{nj}+2e_{25}\right)\left(n\,(n+1)\,(c_{13}+c_{44})\,\eta_{nj} + n\,(n+1)\,(c_{13}-(c_{44}+c_{11}+c_{12}))\right)}. \end{aligned} \tag{34b}$$

The particular solutions of Eqs. (29a), (29b), and (29c) are assumed as

$$u_n^{a,s^p}(r) = D_{n1}^{a,s}\, r^{\beta_{n1}^{a,s}+1} + D_{n2}^{a,s}\, r^{\beta_{n2}^{a,s}+1}, \tag{35a}$$

$$v_n^{a,s^p}(r) = D_{n3}^{a,s}\, r^{\beta_{n1}^{a,s}+1} + D_{n4}^{a,s}\, r^{\beta_{n2}^{a,s}+1}, \tag{35b}$$

$$\varphi_n^{a,s^p}(r) = D_{n5}^{a,s}\, r^{\beta_{n1}^{a,s}+1} + D_{n6}^{a,s}\, r^{\beta_{n2}^{a,s}+1}. \tag{35c}$$

Substituting Eqs. (35) into Eqs. (29) yields

$$\begin{aligned} & d_1^{a,s} D_{n1}^{a,s}\, r^{\beta_{n1}^{a,s}-1} + d_2^{a,s} D_{n2}^{a,s}\, r^{\beta_{n2}^{a,s}-1} + d_3^{a,s} D_{n3}^{a,s}\, r^{\beta_{n1}^{a,s}-1} + d_4^{a,s} D_{n4}^{a,s}\, r^{\beta_{n2}^{a,s}-1} \\ & \quad + d_5^{a,s} D_{n5}^{a,s}\, r^{\beta_{n1}^{a,s}-1} + d_6^{a,s} D_{n6}^{a,s}\, r^{\beta_{n2}^{a,s}-1} = d_7^{a,s}\, r^{\beta_{n1}^{a,s}-1} + d_8^{a,s}\, r^{\beta_{n2}^{a,s}-1}, \end{aligned} \tag{36a}$$

$$\begin{aligned} & d_9^{a,s} D_{n1}^{a,s}\, r^{\beta_{n1}^{a,s}-1} + d_{10}^{a,s} D_{n2}^{a,s}\, r^{\beta_{n2}^{a,s}-1} + d_{11}^{a,s} D_{n3}^{a,s}\, r^{\beta_{n1}^{a,s}-1} + d_{12}^{a,s} D_{n4}^{a,s}\, r^{\beta_{n2}^{a,s}-1} \\ & \quad + d_{13}^{a,s} D_{n5}^{a,s}\, r^{\beta_{n1}^{a,s}-1} + d_{14}^{a,s} D_{n6}^{a,s}\, r^{\beta_{n2}^{a,s}-1} = d_{15}^{a,s}\, r^{\beta_{n1}^{a,s}-1} + d_{16}^{a,s}\, r^{\beta_{n2}^{a,s}-1}, \end{aligned} \tag{36b}$$

$$\begin{aligned} & d_{17}^{a,s} D_{n1}^{a,s}\, r^{\beta_{n1}^{a,s}-1} + d_{18}^{a,s} D_{n2}^{a,s}\, r^{\beta_{n2}^{a,s}-1} + d_{19}^{a,s} D_{n3}^{a,s}\, r^{\beta_{n1}^{a,s}-1} + d_{20}^{a,s} D_{n4}^{a,s}\, r^{\beta_{n2}^{a,s}-1} \\ & \quad + d_{21}^{a,s} D_{n5}^{a,s}\, r^{\beta_{n1}^{a,s}-1} + d_{22}^{a,s} D_{n6}^{a,s}\, r^{\beta_{n2}^{a,s}-1} = d_{23}^{a,s}\, r^{\beta_{n1}^{a,s}-1} + d_{24}^{a,s} r^{\beta_{n2}^{a,s}-1}, \end{aligned} \tag{36c}$$

where the coefficients $d_1^{a,s}$ through $d_{24}^{a,s}$ are presented in Appendix B. Equating the coefficients of identical powers yields

$$d_1^{a,s} D_{n1}^{a,s} + d_3^{a,s} D_{n3}^{a,s} + d_5^{a,s} D_{n5}^{a,s} = d_7^{a,s}, \tag{37a}$$

$$d_9^{a,s} D_{n1}^{a,s} + d_{11}^{a,s} D_{n3}^{a,s} + d_{13}^{a,s} D_{n5}^{a,s} = d_{15}^{a,s}, \tag{37b}$$

$$d_{17}^{a,s} D_{n1}^{a,s} + d_{19}^{a,s} D_{n3}^{a,s} + d_{21}^{a,s} D_{n5}^{a,s} = d_{23}^{a,s}, \tag{37c}$$

$$d_2^{a,s} D_{n2}^{a,s} + d_4^{a,s} D_{n4}^{a,s} + d_6^{a,s} D_{n6}^{a,s} = d_8^{a,s}, \tag{38a}$$

$$d_{10}^{a,s} D_{n2}^{a,s} + d_{12}^{a,s} D_{n4}^{a,s} + d_{14}^{a,s} D_{n6}^{a,s} = d_{16}^{a,s}, \tag{38b}$$

$$d_{18}^{a,s} D_{n2}^{a,s} + d_{20}^{a,s} D_{n4}^{a,s} + d_{22}^{a,s} D_{n6}^{a,s} = d_{24}^{a,s}. \tag{38c}$$

Here, $D_{ni}^{a,s}$ $(i = 1, \ldots, 6)$ are obtained solving the two systems of algebraic equations.

The complete solutions for displacements and electric potential are the sum of Eqs. (33) and (35) and are

$$u_n^{a,s}(r) = \sum_{j=1}^{6} \left(B_{nj}^{a,s}\ r^{\eta_{nj}} \right) + D_{n1}^{a,s}\ r^{\beta_{n1}^{a,s}+1} + D_{n2}^{a,s}\ r^{\beta_{n2}^{a,s}+1}, \tag{39a}$$

$$v_n^{a,s}(r) = \sum_{j=1}^{6} \left(N_{nj} B_{nj}^{a,s}\ r^{\eta_{nj}} \right) + D_{n3}^{a,s}\ r^{\beta_{n1}^{a,s}+1} + D_{n4}^{a,s}\ r^{\beta_{n2}^{a,s}+1}, \tag{39b}$$

$$\varphi_n^{a,s}(r) = \sum_{j=1}^{6} \left(M_{nj} B_{nj}^{a,s}\ r^{\eta_{nj}} \right) + D_{n5}^{a,s}\ r^{\beta_{n1}^{a,s}+1} + D_{n6}^{a,s}\ r^{\beta_{n2}^{a,s}+1}. \tag{39c}$$

For $n = 0$, the system of Navier equations (29) leads to the following single differential equation ($P_0'(\mu) = 0$):

$$\begin{aligned} &\frac{\partial^2 u_0^{a,s}(r)}{\partial r^2} + \frac{2}{r}\frac{\partial u_0^{a,s}(r)}{\partial r} + \frac{2}{r^2}\left(\frac{c_{13} - (c_{11} + c_{12})}{c_{33}}\right) u_0^{a,s}(r) + \frac{e_{22}}{c_{33}}\frac{\partial^2 \varphi_0^{a,s}(r)}{\partial r^2} + \frac{1}{r}\left(\frac{2\,(e_{22} - e_{21})}{c_{33}}\right)\frac{\partial \varphi_0^{a,s}(r)}{\partial r} \\ &= \frac{z_r}{c_{33}}\left((2-f) + \beta_{01}^{a,s}\right) A_{01}^{a,s}\ r^{\beta_{01}^{a,s}-1} + \left((2-f) + \beta_{02}^{a,s}\right) A_{02}^{a,s}\ r^{\beta_{02}^{a,s}-1}, \end{aligned} \tag{40a}$$

$$\begin{aligned} &\frac{\partial^2 u_0^{a,s}(r)}{\partial r^2} + \frac{1}{r}\left(2 + \frac{2e_{21}}{e_{22}}\right)\frac{\partial u_0^{a,s}(r)}{\partial r} + \frac{2}{r^2}\left(\frac{e_{21}}{e_{22}}\right) u_0^{a,s}(r) - \left(\frac{\varepsilon_{22}}{e_{22}}\right)\frac{\partial^2 \varphi_0^{a,s}(r)}{\partial r^2} - \frac{2}{r}\left(\frac{\varepsilon_{22}}{e_{22}}\right)\frac{\partial \varphi_0^{a,s}(r)}{\partial r} \\ &= -\left(\frac{g_{22}}{e_{22}}\right)\left(2 + \beta_{01}^{a,s}\right) A_{01}^{a,s}\ r^{\beta_{01}^{a,s}-1} + \left(2 + \beta_{02}^{a,s}\right) A_{02}^{a,s}\ r^{\beta_{02}^{a,s}-1}. \end{aligned} \tag{40b}$$

This is the system of Euler differential equations. Thus, the solution of homogeneous part of Eqs. (40) may be assumed in the form

$$u_0^{a,s^g}(r) = B_0^{a,s}\ r^{\eta_0}, \tag{41a}$$

$$\varphi_0^{a,s^g}(r) = D_0^{a,s}\ r^{\eta_0}, \tag{41b}$$

where $B_0^{a,s}$, $D_0^{a,s}$, and η_0 are constants to be found using the given boundary conditions. Substituting Eqs. (41) into the homogeneous parts of Eqs. (40) yields

$$\left[\eta_0^2 + 2\eta_0 + \left(\frac{2c_{13} - 2\,(c_{11} + c_{12})}{c_{33}}\right)\right] B_0^{a,s} + \left[\left(\frac{e_{22}}{c_{33}}\right)\eta_0^2 + \left(\frac{2\,(e_{22} - e_{21})}{c_{33}}\right)\eta_0\right] D_0^{a,s} = 0, \tag{42a}$$

$$\left[\eta_0^2 + \left(2 + \frac{2e_{21}}{e_{22}}\right)\eta_0 + \left(\frac{2e_{21}}{e_{22}}\right)\right] B_0^{a,s} - \left[\left(\frac{\varepsilon_{22}}{e_{22}}\right)\eta_0^2 + \left(\frac{2\varepsilon_{22}}{e_{22}}\right)\eta_0\right] D_0^{a,s} = 0. \tag{42b}$$

To obtain the non-trivial solution of the above equation, the determinant of coefficients of the constants $B_0^{a,s}$ and $D_0^{a,s}$ must vanish. This leads to the evaluation of the eigenvector η_0 obtained as

$$\begin{aligned} &-\left(\eta_0^2 + 2\eta_0 + \left(\frac{2c_{13} - 2\,(c_{11} + c_{12})}{c_{33}}\right)\right) \times \left(\left(\frac{\varepsilon_{22}}{e_{22}}\right)\eta_0^2 + \left(\frac{2\varepsilon_{22}}{e_{22}}\right)\eta_0\right) \\ &-\left(\left(\frac{e_{22}}{c_{33}}\right)\eta_0^2 + \left(\frac{2\,(e_{22} - e_{21})}{c_{33}}\right)\eta_0\right) \times \left(\eta_0^2 + \left(2 + \frac{2e_{21}}{e_{22}}\right)\eta_0 + \left(\frac{2e_{21}}{e_{22}}\right)\right) = 0. \end{aligned} \tag{43}$$

Thus, the general solution, utilizing the linearity lemma, is a linear combination of all values of eigenvalues and is obtained as

$$u_0^{a,s^g}(r) = \sum_{j=1}^{4} B_{0j}^{a,s}\ r^{\eta_{0j}}, \quad \varphi_0^{a,s^g}(r) = \sum_{j=1}^{4} M_{0j} B_{0j}^{a,s}\ r^{\eta_{0j}}. \tag{44}$$

The particular solution of Eqs. (40) is assumed as

$$u_0^{a,s^p}(r) = D_{01}^{a,s}\ r^{\beta_{01}^{a,s}+1} + D_{02}^{a,s}\ r^{\beta_{02}^{a,s}+1}, \tag{45a}$$

$$\varphi_0^{a,s^p}(r) = D_{05}^{a,s}\ r^{\beta_{01}^{a,s}+1} + D_{06}^{a,s}\ r^{\beta_{02}^{a,s}+1}. \tag{45b}$$

Substituting Eqs. (45) into Eqs. (40) yields

$$D_{01}^{a,s} = \frac{-\left(d_{011}^{a,s} d_{03}^{a,s} - d_{09}^{a,s} d_{05}^{a,s}\right)}{d_{07}^{a,s} d_{03}^{a,s} - d_{09}^{a,s} d_{01}^{a,s}}, \tag{46a}$$

$$D_{02}^{a,s} = \frac{-(d_{06}^{a,s} d_{010}^{a,s} - d_{04}^{a,s} d_{012}^{a,s})}{d_{02}^{a,s} d_{010}^{a,s} - d_{04}^{a,s} d_{08}^{a,s}}, \tag{46b}$$

$$D_{05}^{a,s} = \frac{-(d_{011}^{a,s} d_{01}^{a,s} - d_{07}^{a,s} d_{05}^{a,s})}{d_{07}^{a,s} d_{03}^{a,s} - d_{09}^{a,s} d_{01}^{a,s}}, \tag{46c}$$

$$D_{06}^{a,s} = \frac{-(d_{06}^{a,s} d_{08}^{a,s} - d_{02}^{a,s} d_{012}^{a,s})}{d_{02}^{a,s} d_{010}^{a,s} - d_{04}^{a,s} d_{08}^{a,s}}, \tag{46d}$$

where the coefficients $d_{01}^{a,s}$ through $d_{012}^{a,s}$ are presented in Appendix B. Here, $D_{0i}^{a,s}\,(i = 1, 2, 5, 6)$ are obtained solving the two systems of algebraic equations.

Thus, the complete solutions for the radial and circumferential displacement components and the electrical potential for all values of n, using Eqs. (39), (44), and (45), are

$$\begin{aligned} u^{a,s}(r,\mu) = &\sum_{j=1}^{4}\left(B_{0j}^{a,s}\, r^{\eta_{0j}}\right) + D_{01}^{a,s}\, r^{\beta_{01}^{a,s}+1} + D_{02}^{a,s}\, r^{\beta_{02}^{a,s}+1} \\ &+ \sum_{n=1}^{\infty}\left[\sum_{j=1}^{6}\left(B_{nj}^{a,s}\, r^{\eta_{nj}}\right) + D_{n1}^{a,s}\, r^{\beta_{n1}^{a,s}+1} + D_{n2}^{a,s}\, r^{\beta_{n2}^{a,s}+1}\right] \times P_n(\mu), \end{aligned} \tag{47}$$

$$v^{a,s}(r,\mu) = \sum_{n=1}^{\infty}\left[\sum_{j=1}^{6}\left(N_{nj} B_{nj}^{a,s}\, r^{\eta_{nj}}\right) + D_{n3}^{a,s}\, r^{\beta_{n1}^{a,s}+1} + D_{n4}^{a,s}\, r^{\beta_{n2}^{a,s}+1}\right] \times P_n'(\mu)\left(1-\mu^2\right)^{\frac{1}{2}}, \tag{48}$$

$$\begin{aligned} \varphi^{a,s}(r,\mu) = &\sum_{j=1}^{4}\left(M_{0j} B_{0j}^{a,s}\, r^{\eta_{0j}}\right) + D_{05}^{a,s}\, r^{\beta_{01}^{a,s}+1} + D_{06}^{a,s}\, r^{\beta_{02}^{a,s}+1} \\ &+ \sum_{n=1}^{\infty}\left[\sum_{j=1}^{6}\left(M_{nj} B_{nj}^{a,s}\, r^{\eta_{nj}}\right) + D_{n5}^{a,s}\, r^{\beta_{n1}^{a,s}+1} + D_{n6}^{a,s}\, r^{\beta_{n2}^{a,s}+1}\right] \times P_n(\mu). \end{aligned} \tag{49}$$

From relations (2), the radial, circumferential and shear stresses, and electrical displacement are obtained as

$$\begin{aligned} \sigma_{rr}^{a,s} = c_{33}\Bigg(&\sum_{j=1}^{4}\left(\eta_{0j}\left(1+\frac{e_{22}}{c_{33}}M_{0j}\right)+\frac{2c_{13}}{c_{33}}\right) B_{0j}^{a,s}\, r^{\eta_{0j}-1} + D_{01}^{a,s}\left(\left(\beta_{01}^{a,s}+1\right)\left(1+\frac{e_{22}}{c_{33}}\frac{D_{05}^{a,s}}{D_{01}^{a,s}}\right)+\frac{2c_{13}}{c_{33}}\right) r^{\beta_{01}^{a,s}} \\ &+ D_{02}^{a,s}\left(\left(\beta_{02}^{a,s}+1\right)\left(1+\frac{e_{22}}{c_{33}}\frac{D_{06}^{a,s}}{D_{02}^{a,s}}\right)+\frac{2c_{13}}{c_{33}}\right) r^{\beta_{02}^{a,s}} - \frac{z_r}{c_{33}}\left(A_{01}^{a,s}\, r^{\beta_{01}^{a,s}} + A_{02}^{a,s}\, r^{\beta_{02}^{a,s}}\right) \\ &+ \Bigg(\sum_{n=1}^{\infty}\sum_{j=1}^{6}\left(\eta_{nj}\left(1+\frac{e_{22}}{c_{33}}M_{nj}\right)+\frac{c_{13}}{c_{33}}\left(2+n\,(n+1)\,N_{nj}\right)\right) B_{nj}^{a,s}\, r^{\eta_{nj}-1} \\ &+ D_{n1}^{a,s}\left(\left(\beta_{n1}^{a,s}+1\right)\left(1+\frac{e_{22}}{c_{33}}\frac{D_{n5}^{a,s}}{D_{n1}^{a,s}}\right)+\frac{c_{13}}{c_{33}}\left(2+n\,(n+1)\,N_{nj}\frac{D_{n3}^{a,s}}{D_{n1}^{a,s}}\right)\right) r^{\beta_{n1}^{a,s}} \\ &+ D_{n2}^{a,s}\left(\left(\beta_{n2}^{a,s}+1\right)\left(1+\frac{e_{22}}{c_{33}}\frac{D_{n6}^{a,s}}{D_{n2}^{a,s}}\right)+\frac{c_{13}}{c_{33}}\left(2+n\,(n+1)\,N_{nj}\frac{D_{n4}^{a,s}}{D_{n2}^{a,s}}\right)\right) r^{\beta_{n2}^{a,s}} \\ &- \frac{z_r}{c_{33}}\left(A_{n1}^{a,s}\, r^{\beta_{n1}^{a,s}} + A_{n2}^{a,s}\, r^{\beta_{n2}^{a,s}}\right)\Bigg) \times P_n(\mu)\Bigg), \end{aligned} \tag{50}$$

$$\sigma_{r\theta}^{a,s} = c_{44}\left(\sum_{n=1}^{\infty}\left[\sum_{j=1}^{6} B_{nj}^{a,s}\left(N_{nj}\ \left(\eta_{nj}-1\right)+\frac{e_{25}}{c_{44}}M_{nj}-1\right)+\right] r^{\eta_{nj}-1}\right.$$
$$+ D_{n1}^{a,s}\left(\frac{e_{25}}{c_{44}}\frac{D_{n5}^{a,s}}{D_{n1}^{a,s}}+\frac{D_{n3}^{a,s}}{D_{n1}^{a,s}}\beta_{n1}^{a,s}-1\right) r^{\beta_{n1}^{a,s}}$$
$$\left.+D_{n2}^{a,s}\left(\frac{e_{25}}{c_{44}}\frac{D_{n6}^{a,s}}{D_{n2}^{a,s}}+\frac{D_{n4}^{a,s}}{D_{n2}^{a,s}}\beta_{n1}^{a,s}-1\right) r^{\beta_{n1}^{a,s}}\times P_n'(\mu)\left(1-\mu^2\right)^{\frac{1}{2}}\right), \tag{51}$$

$$\sigma_{\theta\theta}^{a,s} = c_{13}\left(\sum_{j=1}^{4}\left(\eta_{0j}\left(1+\frac{e_{21}}{c_{13}}M_{0j}\right)+\frac{c_{11}+c_{12}}{c_{13}}\right)B_{0j}^{a,s}\ r^{\eta_{0j}-1}\right.$$
$$+ D_{01}^{a,s}\left(\left(\beta_{01}^{a,s}+1\right)\left(1+\frac{e_{21}}{c_{13}}\frac{D_{05}^{a,s}}{D_{01}^{a,s}}\right)+\frac{c_{11}+c_{12}}{c_{13}}\right) r^{\beta_{01}^{a,s}}$$
$$+ D_{02}^{a,s}\left(\left(\beta_{02}^{a,s}+1\right)\left(1+\frac{e_{21}}{c_{13}}\frac{D_{06}^{a,s}}{D_{02}^{a,s}}\right)+\frac{c_{11}+c_{12}}{c_{13}}\right) r^{\beta_{02}^{a,s}}-\frac{z_\theta}{c_{13}}\left(A_{01}^{a,s}\ r^{\beta_{01}^{a,s}}+A_{02}^{a,s}\ r^{\beta_{02}^{a,s}}\right)$$
$$+\left(\sum_{n=1}^{\infty}\sum_{j=1}^{6}\left(\eta_{nj}\left(1+\frac{e_{21}}{c_{13}}M_{nj}\right)+\frac{c_{11}+c_{12}}{c_{13}}\right)B_{nj}^{a,s}\ r^{\eta_{nj}-1}\right.$$
$$+ D_{n1}^{a,s}\left(\left(\beta_{n1}^{a,s}+1\right)\left(1+\frac{e_{21}}{c_{13}}\frac{D_{n5}^{a,s}}{D_{n1}^{a,s}}\right)+\frac{c_{11}+c_{12}}{c_{13}}\right) r^{\beta_{n1}^{a,s}}$$
$$\left.+D_{n2}^{a,s}\left(\left(\beta_{n2}^{a,s}+1\right)\left(1+\frac{e_{21}}{c_{13}}\frac{D_{n6}^{a,s}}{D_{n2}^{a,s}}\right)+\frac{c_{11}+c_{12}}{c_{13}}\right) r^{\beta_{n2}^{a,s}}-\frac{z_r}{c_{33}}\left(A_{n1}^{a,s}\ r^{\beta_{n1}^{a,s}}+A_{n2}^{a,s}\ r^{\beta_{n2}^{a,s}}\right)\right)P_n(\mu)\Bigg)$$
$$+ c_{13}\left(\sum_{n=1}^{\infty}\left[\sum_{j=1}^{6}\left(N_{nj}B_{nj}^{a,s}\ r^{\eta_{nj-1}}\right)+D_{n3}^{a,s}\ r^{\beta_{n1}^{a,s}+1}+D_{n4}^{a,s}\ r^{\beta_{n2}^{a,s}+1}\right]\right.$$
$$\left.\times\left[\frac{c_{11}}{c_{13}}n\left(n+1\right)P_n(\mu)+\frac{c_{12}-c_{11}}{c_{13}}\mu P_n'(\mu)\right]\right), \tag{52}$$

$$D_{rr}^{a,s} = e_{22}\left(\sum_{j=1}^{4}\left(\eta_{0j}\left(1-\frac{\varepsilon_{22}}{e_{22}}M_{0j}\right)+\frac{2e_{21}}{e_{22}}\right)B_{0j}^{a,s}\ r^{\eta_{0j}-1}\right.$$
$$+D_{01}^{a,s}\left(\left(\beta_{01}^{a,s}+1\right)\left(1-\frac{\varepsilon_{22}}{e_{22}}\frac{D_{05}^{a,s}}{D_{01}^{a,s}}\right)+\frac{2e_{21}}{e_{22}}\right) r^{\beta_{01}^{a,s}}$$
$$+ D_{02}^{a,s}\left(\left(\beta_{02}^{a,s}+1\right)\left(1-\frac{\varepsilon_{22}}{e_{22}}\frac{D_{06}^{a,s}}{D_{02}^{a,s}}\right)+\frac{2e_{21}}{e_{22}}\right) r^{\beta_{02}^{a,s}}+\frac{g_{22}}{e_{22}}\left(A_{01}^{a,s}\ r^{\beta_{01}^{a,s}}+A_{02}^{a,s}\ r^{\beta_{02}^{a,s}}\right)$$
$$+\sum_{n=1}^{\infty}\left(\sum_{j=1}^{6}\left(\eta_{nj}\left(1-\frac{\varepsilon_{22}}{e_{22}}M_{nj}\right)+\frac{e_{21}}{e_{22}}\left(2+n\left(n+1\right)N_{nj}\right)\right)B_{nj}^{a,s}r^{\eta_{nj}-1}\right.$$
$$+ D_{n1}^{a,s}\left(\left(\beta_{n1}^{a,s}+1\right)\left(1-\frac{\varepsilon_{22}}{e_{22}}\frac{D_{n5}^{a,s}}{D_{n1}^{a,s}}\right)+\frac{e_{21}}{e_{22}}\left(2+\frac{D_{n3}^{a,s}}{D_{n1}^{a,s}}n\left(n+1\right)\right)\right) r^{\beta_{n1}^{a,s}}$$
$$+D_{n2}^{a,s}\left(\left(\beta_{n2}^{a,s}+1\right)\left(1-\frac{\varepsilon_{22}}{e_{22}}\frac{D_{n6}^{a,s}}{D_{n2}^{a,s}}\right)+\frac{e_{21}}{e_{22}}\left(2+\frac{D_{n4}^{a,s}}{D_{n2}^{a,s}}n\left(n+1\right)\right)\right) r^{\beta_{n2}^{a,s}}$$
$$\left.+\frac{g_{22}}{e_{22}}\left(A_{n1}^{a,s}\ r^{\beta_{n1}^{a,s}}+A_{n2}^{a,s}\ r^{\beta_{n2}^{a,s}}\right)\right)\times P_n(\mu)\Bigg), \tag{53}$$

$$D_{\theta\theta}^{a,s} = e_{25}\left(\sum_{n=1}^{\infty}\left(\sum_{j=1}^{6} B_{nj}^{a,s}\left(N_{nj}\left(\eta_{nj}-1\right)-\frac{\varepsilon_{11}}{e_{25}}M_{nj}-1\right)r^{\eta_{nj}-1}\right.\right.$$
$$+ D_{n1}^{a,s}\left(\beta_{n1}^{a,s}\frac{D_{n3}^{a,s}}{D_{n1}^{a,s}}-\frac{\varepsilon_{11}}{e_{25}}\frac{D_{n5}^{a,s}}{D_{n1}^{a,s}}-1\right)r^{\beta_{n1}^{a,s}}$$
$$\left.\left.+D_{n2}^{a,s}\left(\beta_{n2}^{a,s}\frac{D_{n4}^{a,s}}{D_{n2}^{a,s}}-\frac{\varepsilon_{11}}{e_{25}}\frac{D_{n6}^{a,s}}{D_{n2}^{a,s}}-1\right)r^{\beta_{n2}^{a,s}}\right)\times P_n'(\mu)\left(1-\mu^2\right)^{\frac{1}{2}}\right)$$
$$+ g_{21}\left(\sum_{n=0}^{\infty}\left(A_{n1}^{a,s}\,r^{\beta_{n1}^{a,s}}+A_{n2}^{a,s}\,r^{\beta_{n2}^{a,s}}\right)\times P_n(\mu)\right). \tag{54}$$

4.2 FGM layer

The solution of the Navier equations (12) is assumed in the form of Legendre series as

$$u^F(r,\mu) = \sum_{n=0}^{\infty} u_n^F(r)P_n(\mu), \tag{55a}$$
$$v^F(r,\mu) = \sum_{n=0}^{\infty} v_n^F(r)P_n'(\mu)\left(1-\mu^2\right)^{\frac{1}{2}}, \tag{55b}$$

where $u_n^F(r)$ and $v_n^F(r)$ are functions of r. Substituting Eqs. (23) and (55) into Eqs. (12) and then using the method given in Appendix A to separate the independent variables r and μ leads to

$$\frac{\partial^2 u_n^F(r)}{\partial r^2}+\frac{(2+m_1)}{r}\frac{\partial u_n^F(r)}{\partial r}+\frac{1}{r^2}\left(\frac{2\nu}{1-\nu}m_1-n\,(n+1)\,\frac{1-2\nu}{2-2\nu}-2\right)u_n^F(r)$$
$$+\frac{n\,(n+1)}{2r(1-\nu)}\frac{\partial v_n^F(r)}{\partial r}+\frac{n\,(n+1)}{r^2}\left(\frac{\nu}{1-\nu}m_1-\frac{3-4\nu}{2-2\nu}\right)v_n^F(r)$$
$$=\frac{1+\nu}{1-\nu}\alpha_0\left(\left(m_1+m_2+\beta_{n1}^F\right)A_{n1}^F\,r^{\beta_{n1}^F+m_2-1}+\left(m_1+m_2+\beta_{n2}^F\right)A_{n2}^F\,r^{\beta_{n2}^F+m_2-1}\right), \tag{56a}$$
$$\frac{\partial^2 v_n^F(r)}{\partial r^2}+\frac{(2+m_1)}{r}\frac{\partial v_n^F(r)}{\partial r}-\frac{1}{r^2}\left(m_1+n\,(n+1)\,\frac{2-2\nu}{1-2\nu}\right)v_n^F(r)$$
$$-\frac{1}{r\,(1-2\nu)}\frac{\partial u_n^F(r)}{\partial r}-\frac{1}{r^2}\left(m_1+\frac{4-4\nu}{1-2\nu}\right)u_n^F(r)$$
$$=-\frac{1+\nu}{1-2\nu}\alpha_0\left(A_{n1}^F\,r^{\beta_{n1}^F+m_2-1}+A_{n2}^F\,r^{\beta_{n2}^F+m_2-1}\right). \tag{56b}$$

Thus, the solution of homogeneous part of the system of Euler differential equations (56) may be assumed in the form

$$u_n^{Fg}(r) = B^F r^{\gamma}, \tag{57a}$$
$$v_n^{Fg}(r) = C^F r^{\gamma}. \tag{57b}$$

Here, B^F and C^F are constants to be found using the given boundary conditions. Substituting Eqs. (57) into the homogeneous parts of Eqs. (56) yields

$$\left(\gamma^2+(m_1+1)\,\gamma+\frac{2\nu m_1}{1-\nu}-n\,(n+1)\,\frac{1-2\nu}{2-2\nu}-2\right)B^F+\frac{n\,(n+1)}{2-2\nu}\left(\gamma+2\nu m_1-3+4\nu\right)C^F=0, \tag{58a}$$

$$\frac{-1}{1-2\nu}\left(\gamma+(1-2\nu)\,m_1+4-4\nu\right)B^F+\left(\gamma^2+(m_1+1)\,\gamma-m_1-n\,(n+1)\,\frac{2-2\nu}{1-2\nu}\right)C^F=0. \tag{58b}$$

Equations (58) are a system of algebraic equations such that for obtaining their non-trivial solution, their determinant should be equal to zero, and their four roots are evaluated as follows:

$$\left(\gamma^2+(m_1+1)\,\gamma+\frac{2\nu m_1}{1-\nu}-n\,(n+1)\,\frac{1-2\nu}{2-2\nu}-2\right)\times\left(\gamma^2+(m_1+1)\,\gamma-m_1-n\,(n+1)\,\frac{2-2\nu}{1-2\nu}\right)$$
$$+\frac{n\,(n+1)}{(2-2\nu)\,(1-2\nu)}\,(\gamma+2\nu m_1-3+4\nu)\times(\gamma+(1-2\nu)\,m_1+4-4\nu)=0. \tag{59}$$

Therefore,

$$u_n^{Fg}(r)=\sum_{j=1}^{4}B_{nj}^F\,r^{\gamma_{nj}},\quad v_n^{Fg}(r)=\sum_{j=1}^{4}N_{nj}\,B_{nj}^F r^{\gamma_{nj}}, \tag{60}$$

where

$$N_{nj}=\frac{\left(\gamma_{nj}^2+(m_1+1)\,\gamma_{nj}+\frac{2\nu m_1}{1-\nu}-n\,(n+1)\,\frac{1-2\nu}{2-2\nu}-2\right)}{-\frac{n(n+1)}{2-2\nu}\left(\gamma_{nj}+2\nu m_1-3+4\nu\right)}. \tag{61}$$

The particular solutions of Eqs. (56) are assumed to be as follows:

$$u_n^{Fp}(r)=D_{n1}^F\,r^{\beta_{n1}^F+m_2+1}+D_{n2}^F\,r^{\beta_{n2}^F+m_2+1}, \tag{62a}$$
$$v_n^{Fp}(r)=D_{n3}^F\,r^{\beta_{n1}^F+m_2+1}+D_{n4}^F\,r^{\beta_{n2}^F+m_2+1}. \tag{62b}$$

Substituting Eqs. (62) into Eqs. (56) yields

$$d_1^F D_{n1}^F\,r^{\beta_{n1}^F+m_2-1}+d_2^F D_{n2}^F\,r^{\beta_{n2}^F+m_2-1}+d_3^F D_{n3}^F\,r^{\beta_{n1}^F+m_2-1}+d_4^F D_{n4}^F\,r^{\beta_{n2}^F+m_2-1}$$
$$=d_5^F\,r^{\beta_{n1}^F+m_2-1}+d_6^F\,r^{\beta_{n2}^F+m_2-1}, \tag{63a}$$
$$d_7^F D_{n1}^F\,r^{\beta_{n1}^F+m_2-1}+d_8^F D_{n2}^F\,r^{\beta_{n2}^F+m_2-1}+d_9^F D_{n3}^F\,r^{\beta_{n1}^F+m_2-1}+d_{10}^F D_{n4}^F\,r^{\beta_{n2}^F+m_2-1}$$
$$=d_{11}^F\,r^{\beta_{n1}^F+m_2-1}+d_{12}^F\,r^{\beta_{n2}^F+m_2-1}, \tag{63b}$$

where the coefficients d_1^F through d_{12}^F are presented in Appendix C. Equating the coefficients of identical powers yields

$$\begin{cases} d_1^F D_{n1}^F+d_3^F D_{n3}^F=d_5^F,\\ d_7^F D_{n1}^F+d_9^F D_{n3}^F=d_{11}^F, \end{cases} \tag{64}$$

$$\begin{cases} d_2^F D_{n2}^F+d_4^F D_{n4}^F=d_6^F,\\ d_8^F D_{n2}^F+d_{10}^F D_{n4}^F=d_{12}^F. \end{cases} \tag{65}$$

Here, $D_{ni}^{a,s}$ $(i=1,\ldots,4)$ are obtained solving the two systems of algebraic equations.

The complete solutions for displacements are the sum of Eqs. (60) and (62) and are

$$u_n^F(r)=\sum_{j=1}^{4}\left(B_{nj}^F\,r^{\gamma_{nj}}\right)+D_{n1}^F\,r^{\beta_{n1}^F+m_2+1}+D_{n2}^F\,r^{\beta_{n2}^F+m_2+1}, \tag{66}$$

$$v_n^F(r)=\sum_{j=1}^{4}\left(N_{nj}B_{nj}^F\,r^{\gamma_{nj}}\right)+D_{n3}^F\,r^{\beta_{n1}^F+m_2+1}+D_{n4}^F\,r^{\beta_{n2}^F+m_2+1}. \tag{67}$$

For $n=0$ $(P_0'(\mu)=0)$, the system of Navier equations (56) leads to the following single differential equation:

$$\frac{\partial^2 u_0^F(r)}{\partial r^2}+\frac{(2+m_1)}{r}\frac{\partial u_0^F(r)}{\partial r}+\frac{1}{r^2}\left(\frac{2\nu m_1}{1-\nu}-2\right)u_0^F(r)$$
$$=\frac{1+\nu}{1-\nu}\alpha_0\left(\left(m_1+m_2+\beta_{01}^F\right)A_{01}^F\,r^{\beta_{01}^F+m_2-1}+\left(m_1+m_2+\beta_{02}^F\right)A_{02}^F\,r^{\beta_{02}^F+m_2-1}\right). \tag{68}$$

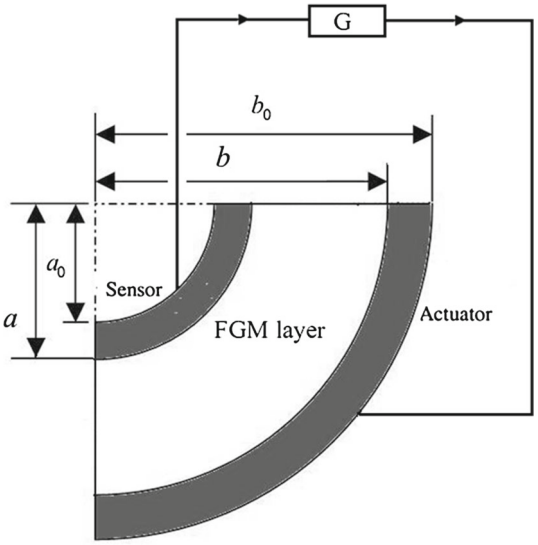

Fig. 1 Schematic diagram showing the feedback configuration and geometry of the FGM hollow sphere with piezoelectric sensor/actuator layers

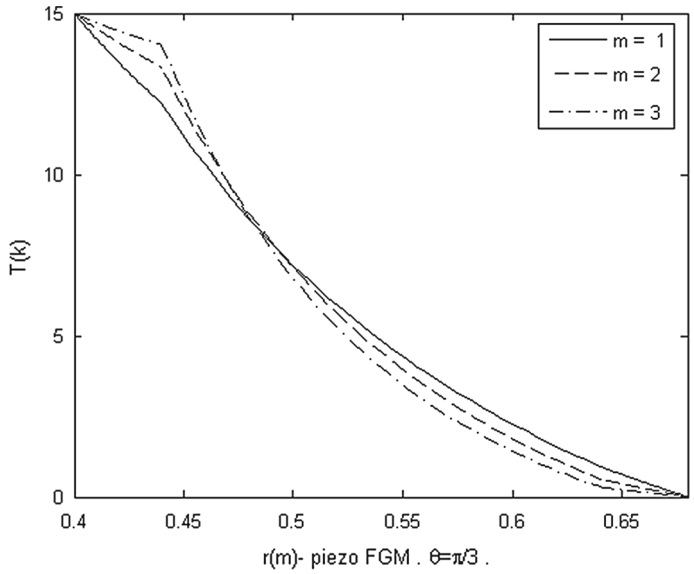

Fig. 2 Temperature distribution in the piezo-FGM hollow sphere with various m, at $\theta = \pi/3$

Solving the homogeneous and non-homogeneous parts of Eq. (68) provides the complete solution for $u_0^F(r)$ as

$$u_0^F(r) = \sum_{j=1}^{2} \left(B_{0j}^F \, r^{\gamma_{0j}} \right) + D_{01}^F \, r^{\beta_{01}^F + m_2 + 1} + D_{02}^F \, r^{\beta_{02}^F + m_2 + 1}, \tag{69}$$

where

$$\gamma_{0j} = \frac{-(m_1+1)}{2} \pm \left(\frac{(m_1+1)^2}{4} + \frac{2\nu m_1}{1-\nu} - 2 \right)^{\frac{1}{2}}, \tag{70}$$

$$D_{0j}^F = \frac{(1+\nu)\left(m_1 + m_2 + \beta_{0j}^F\right)\alpha_0 A_{0j}^F}{(1-\nu)\left(\left(2 + m_1 + m_2 + \beta_{0j}^F\right)\left(1 + m_2 + \beta_{0j}^F\right) + \frac{2\nu m_1}{1-\nu} - 2\right)}. \tag{71}$$

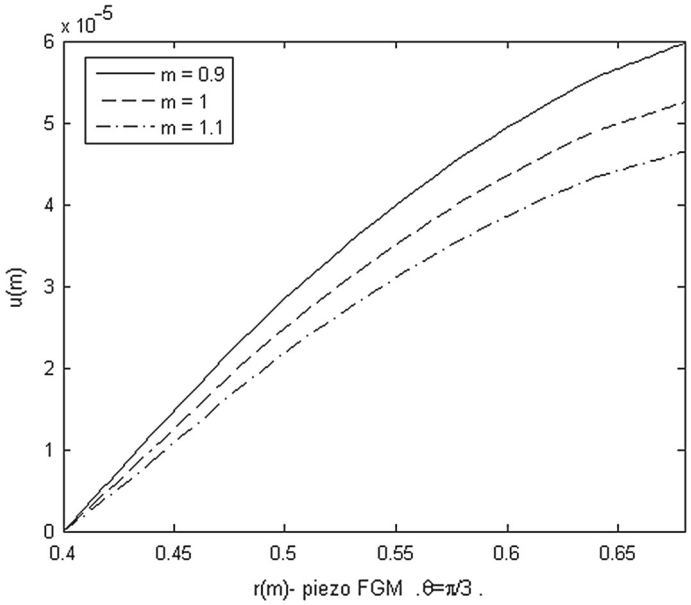

Fig. 3 Radial displacement distribution in the piezo-FGM hollow sphere with various m, at $\theta = \pi/3$

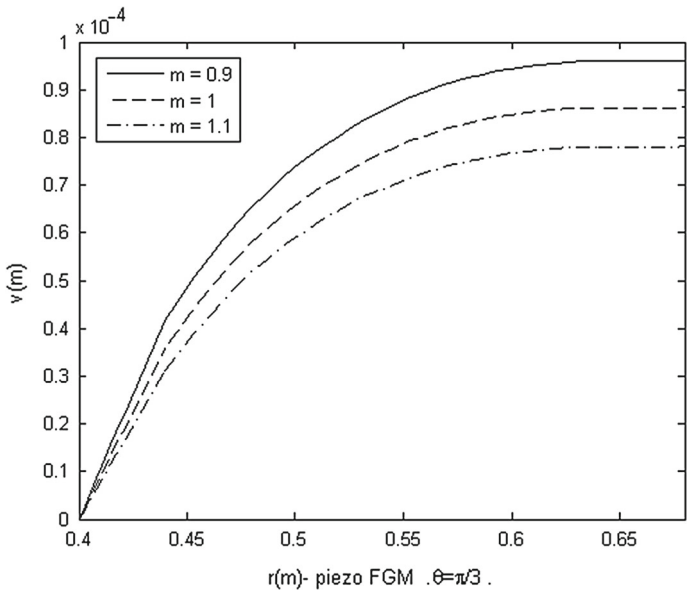

Fig. 4 Circumferential displacement distribution in the piezo-FGM hollow sphere with various m, at $\theta = \pi/3$

Thus, the complete solution of radial and circumferential displacement components for all values of n using Eqs. (66) and (69) is

$$u^F(r,\mu) = \sum_{j=1}^{2}\left(B_{0j}^F\, r^{\gamma_{0j}}\right) + D_{01}^F\, r^{\beta_{01}^F+m_2+1} + D_{02}^F\, r^{\beta_{02}^F+m_2+1} + \sum_{n=1}^{\infty}\left[\sum_{j=1}^{4}\left(B_{nj}^F r^{\gamma_{nj}}\right) + D_{n1}^F\, r^{\beta_{n1}^F+m_2+1} + D_{n2}^F\, r^{\beta_{n2}^F+m_2+1}\right] \times P_n(\mu), \tag{72}$$

$$v^F(r,\mu) = \sum_{n=1}^{\infty}\left[\sum_{j=1}^{4}\left(N_{nj}\, B_{nj}^F r^{\gamma_{nj}}\right) + D_{n3}^F\, r^{\beta_{n1}^F+m_2+1} + D_{n4}^F\, r^{\beta_{n2}^F+m_2+1}\right] P_n'(\mu)\left(1-\mu^2\right)^{\frac{1}{2}}. \tag{73}$$

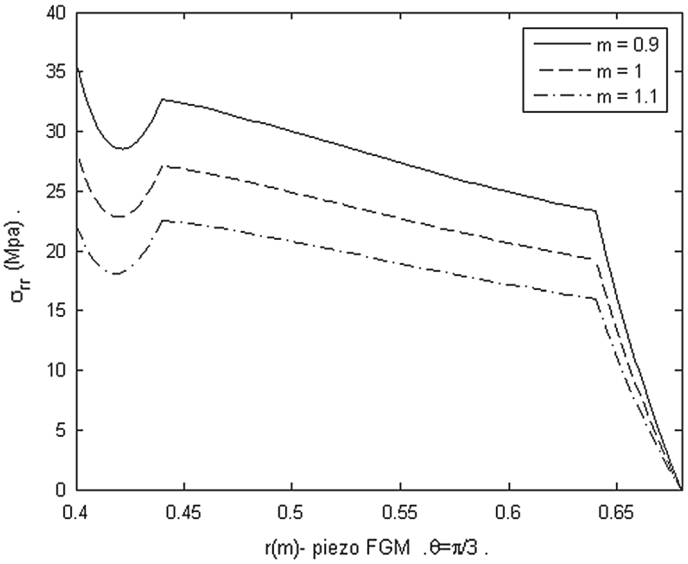

Fig. 5 Radial stress distribution in the piezo-FGM hollow sphere with various m, at $\theta = \pi/3$

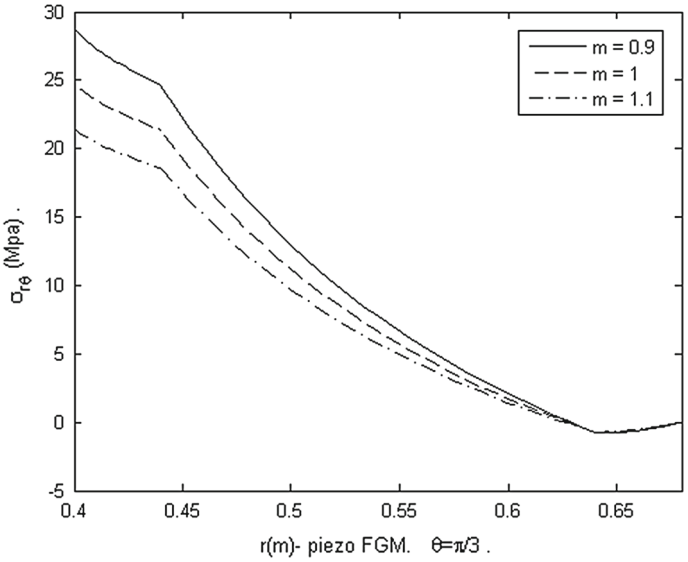

Fig. 6 Shear stress distribution in the piezo-FGM hollow sphere with various m, at $\theta = \pi/3$

From the stress–strain relations (2), the radial, circumferential, and shear stresses are obtained as

$$\begin{aligned}\sigma_{rr}^{F} = \frac{E_0}{(1+\nu)(1-2\nu)} \Bigg(& \sum_{j=1}^{2} \Big(\left(2\nu + (1-\nu)\gamma_{0j}\right) B_{0j}^{F}\, r^{\gamma_{0j}+m_1-1} \\ & + D_{0j}^{F} \left(2\nu + (1-\nu)(\gamma_{0j}+m_2+1)\right) r^{\beta_{0j}^{F}+m_1+m_2} \Big) \\ & - \alpha_0 (1+\nu) \left(A_{01}^{F}\, r^{\beta_{01}^{F}+m_1+m_2} + A_{02}^{F}\, r^{\beta_{02}^{F}+m_1+m_2} \right) \\ & + \Bigg(\sum_{n=1}^{\infty} \Bigg[\sum_{j=1}^{4} \left(2\nu + (1-\nu)\gamma_{nj} + n(n+1)\nu N_{nj}\right) B_{nj}^{F}\, r^{\gamma_{nj}+m_1-1} \\ & + \left(\left(2\nu + (1-\nu)\left(\beta_{n1}^{F}+m_2+1\right)\right) D_{n1}^{F} + n(n+1)\nu D_{n3}^{F} \right) r^{\beta_{n1}^{F}+m_1+m_2}\end{aligned}$$

$$+\left(\left(2\nu+(1-\nu)\left(\beta_{n2}^{F}+m_2+1\right)\right)D_{n2}^{F}+n(n+1)\nu D_{n4}^{F}\right)\ r^{\beta_{n2}^{F}+m_1+m_2}\Bigg]\Bigg)\times P_n(\mu)\Bigg)$$

$$-\frac{E_0\alpha_0\,(1+\nu)}{(1+\nu)\,(1-2\nu)}\left(\sum_{n=1}^{\infty}\left(A_{n1}^{F}\ r^{\beta_{n1}^{F}+m_1+m_2}+A_{n2}^{F}\ r^{\beta_{n2}^{F}+m_1+m_2}\right)\times P_n(\mu)\right), \tag{74}$$

$$\sigma_{r\theta}^{F}=\frac{E_0}{2\,(1+\nu)}\left(\sum_{n=1}^{\infty}\left[\sum_{j=1}^{4}\left(N_{nj}\left(\gamma_{nj}-1\right)-1\right)B_{nj}^{F}\ r^{\gamma_{nj}+m_1-1}-\left(D_{n1}^{F}-\left(\beta_{n1}^{F}+m_2\right)D_{n3}^{F}\right)\ r^{\beta_{n1}^{F}+m_1+m_2}\right.\right.$$

$$\left.\left.-\left(D_{n2}^{F}-\left(\beta_{n2}^{F}+m_2\right)D_{n4}^{F}\right)\ r^{\beta_{n2}^{F}+m_1+m_2}\right]\times P_n'(\mu)\left(1-\mu^2\right)^{\frac{1}{2}}\right), \tag{75}$$

$$\sigma_{\theta\theta}^{F}=\frac{E_0}{(1+\nu)\,(1-2\nu)}\left(\sum_{j=1}^{2}\left(\left(1+\nu\gamma_{0j}\right)B_{0j}^{F}\ r^{\gamma_{0j}+m_1-1}+(1+\nu)\left(\gamma_{0j}+m_2+1\right)D_{0j}^{F}\ r^{\beta_{0j}^{F}+m_1+m_2}\right)\right.$$

$$-\alpha_0\,(1+\nu)\left(A_{01}^{F}\ r^{\beta_{01}^{F}+m_1+m_2}+A_{02}^{F}\ r^{\beta_{02}^{F}+m_1+m_2}\right)$$

$$+\sum_{n=1}^{\infty}\left[\sum_{j=1}^{4}\left(1+\nu\gamma_{nj}\right)B_{nj}^{F}\ r^{\gamma_{nj}+m_1-1}+(1+\nu)\left(\beta_{n1}^{F}+m_2+1\right)D_{n1}^{F}\ r^{\beta_{n1}^{F}+m_1+m_2}\right.$$

$$+(1+\nu)\left(\beta_{n2}^{F}+m_2+1\right)D_{n2}^{F}\ r^{\beta_{n2}^{F}+m_1+m_2}-\alpha_0\,(1+\nu)$$

$$\left.\left.\times\left(A_{n1}^{F}\ r^{\beta_{n1}^{F}+m_1+m_2}+A_{n2}^{F}\ r^{\beta_{n2}^{F}+m_1+m_2}\right)\right]\times P_n(\mu)\right)$$

$$+\frac{E_0}{(1+\nu)\,(1-2\nu)}\left(\sum_{n=1}^{\infty}\left[\sum_{j=1}^{4}N_{nj}B_{nj}^{F}\ r^{\gamma_{nj}+m_1-1}+D_{n3}^{F}\ r^{\beta_{n1}^{F}+m_1+m_2}+D_{n4}^{F}\ r^{\beta_{n2}^{F}+m_1+m_2}\right]\right.$$

$$\left.\times\left[\left(n^2+n\right)(1-\nu)\,P_n(\mu)-(1-2\nu)\,\mu P_n'(\mu)\right]\right). \tag{76}$$

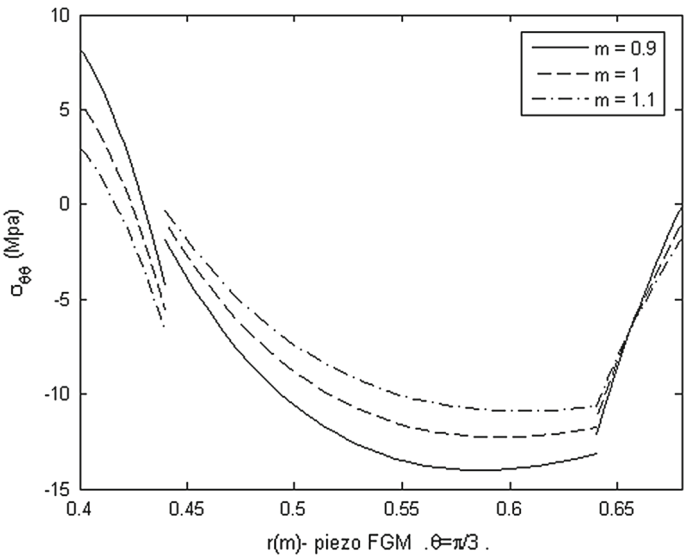

Fig. 7 Circumferential stress distribution in the piezo-FGM hollow sphere with various m, at $\theta=\pi/3$

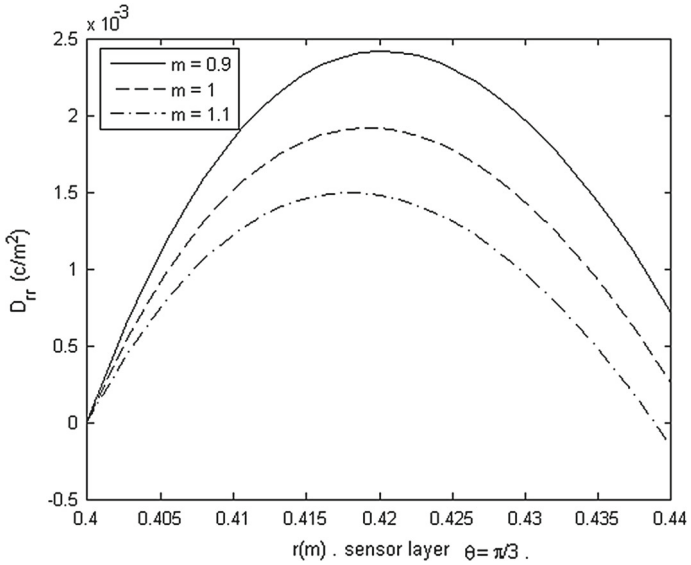

Fig. 8 Radial electrical displacement in the sensor layer with various m, at $\theta = \pi/3$

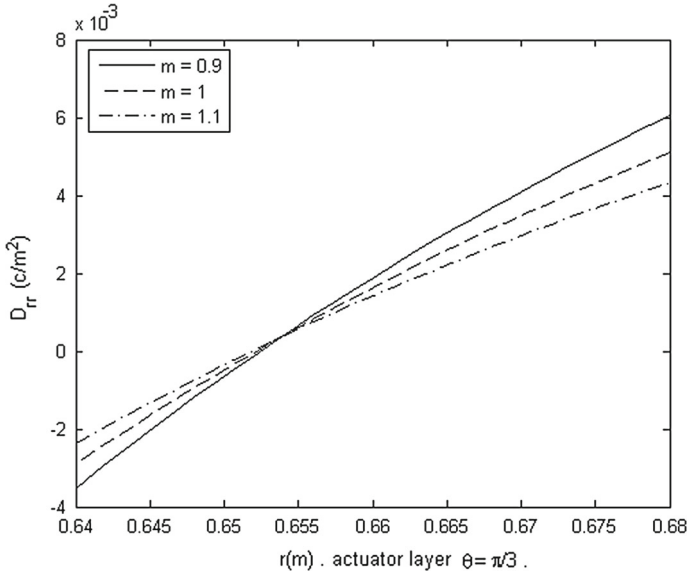

Fig. 9 Radial electrical displacement in the actuator layer with various m, at $\theta = \pi/3$

4.3 Boundary and continuity conditions

It is obvious that the unknown parameters B_{nj}^{F} $(j = 1, \ldots, 4)$ and $B_{nj}^{a,s}(j = 1, \ldots, 6)$ (16 unknown constants) can be evaluated by satisfying the boundary conditions and continuity requirements on the interface. Therefore, displacements, electric potential, stress, and other responses can be evaluated. The corresponding boundary conditions can be selected from the following general mechanical boundary conditions

$$u^s(a_0,\theta) = R_1 P_n(\cos\theta), \quad v^s(a_0,\theta) = R_2 P_n(\cos\theta),$$
$$\sigma_{rr}^s(a_0,\theta) = R_3 P_n(\cos\theta), \quad \sigma_{r\theta}^s(a_0,\theta) = R_4 P_n(\cos\theta), \tag{77a}$$
$$u^a(b_0,\theta) = R_5 P_n(\cos\theta), \quad v^a(b_0,\theta) = R_6 P_n(\cos\theta),$$
$$\sigma_{rr}^a(b_0,\theta) = R_7 P_n(\cos\theta), \quad \sigma_{r\theta}^a(b_0,\theta) = R_8 P_n(\cos\theta), \tag{77b}$$

where R_1 through R_8 are some known constant coefficients.

Furthermore, for electrical boundary conditions, we have:

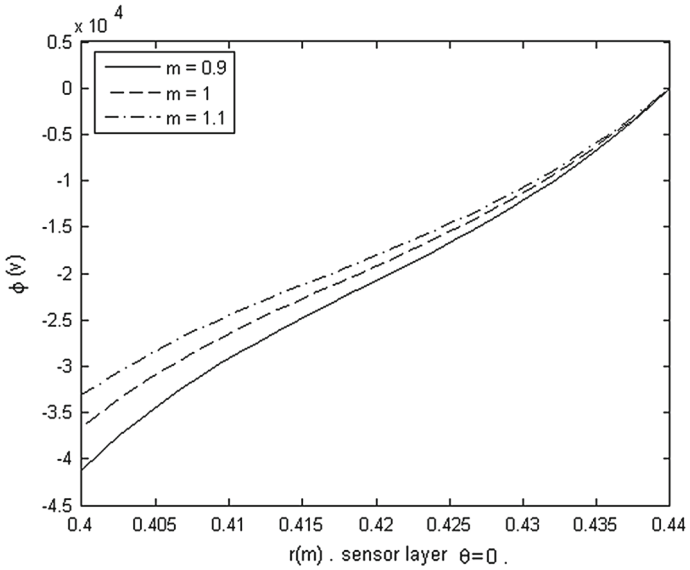

Fig. 10 Electric potential distribution in the sensor layer with various m, at $\theta = 0$

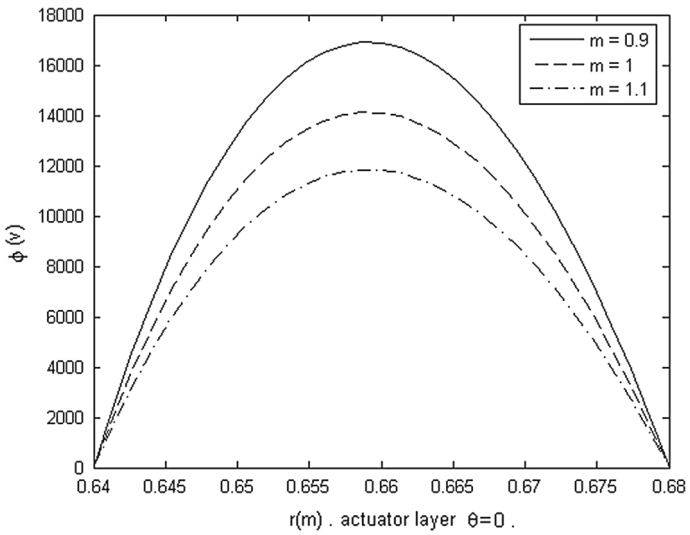

Fig. 11 Electric potential distribution in the actuator layer with various m, at $\theta = 0$

For the sensor layer,

$$D_{rr}^{s}(a_0, \theta) = 0, \quad \varphi^{s}(a, \theta) = 0; \tag{78}$$

For the actuator layer,

$$\varphi^{a}(b, \theta) = 0\,, \quad \varphi^{a}(b_0, \theta) = V^{a} P_n(\cos\theta)\,. \tag{79}$$

$V^{a} P_n(\cos\theta)$ is the input voltage to the actuator layer that can be obtained as follows:

$$V^{a} P_n(\cos\theta) = G\ V^{s} P_n(\cos\theta). \tag{80}$$

Here, G is the feedback gain, and $V^{s} P_n(\cos\theta)$ is the output voltage of the sensor layer:

$$\varphi^{s}(a_0, \theta) = V^{s} P_n(\cos\theta)\,. \tag{81}$$

In fact, the sensor output is used to determine the input to the actuator using the feedback gain control algorithm (see Fig. 1).

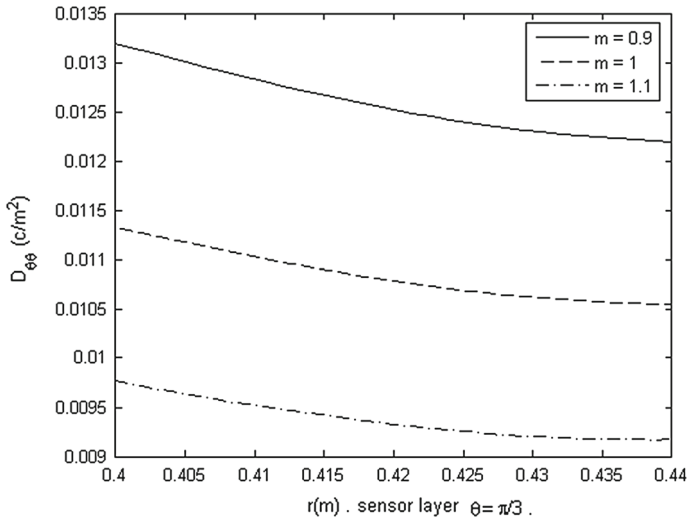

Fig. 12 Circumferential electrical displacement in the sensor layer with various m, at $\theta = \pi/3$

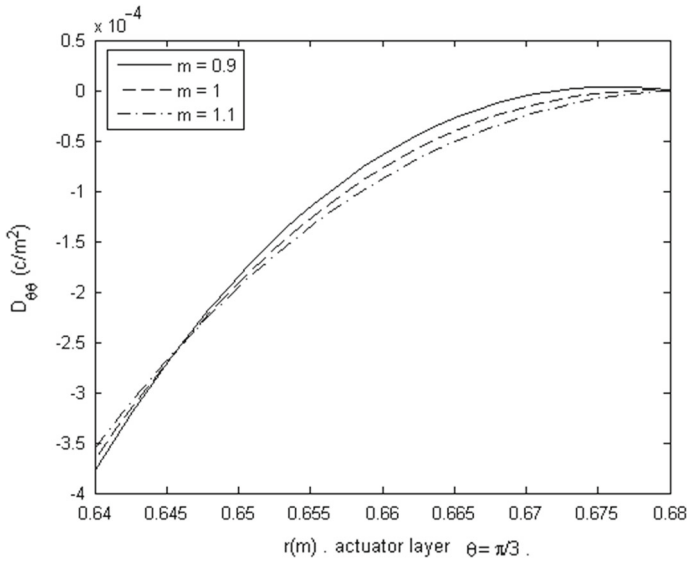

Fig. 13 Circumferential electrical displacement in the actuator layer with various m, at $\theta = \pi/3$

In addition, the continuity requirements for the stresses and displacements on the interfaces must be satisfied; therefore, we have

$$u^s(a,\theta) = u^F(a,\theta),\quad v^s(a,\theta) = v^F(a,\theta),\quad \sigma^s_{rr}(a,\theta) = \sigma^F_{rr}(a,\theta),\quad \sigma^s_{r\theta}(a,\theta) = \sigma^F_{r\theta}(a,\theta), \tag{82a}$$

$$u^F(b,\theta) = u^a(b,\theta),\quad v^F(b,\theta) = v^a(b,\theta),\quad \sigma^F_{rr}(b,\theta) = \sigma^a_{rr}(b,\theta),\quad \sigma^F_{r\theta}(b,\theta) = \sigma^a_{r\theta}(b,\theta). \tag{82b}$$

5 Numerical results and discussion

The analytical solutions obtained in the previous section may be checked for two examples. Then, consider a thick smart FGM hollow sphere (Fig. 1) with the following geometry properties:

$$a_0 = 0.40\,\text{m},\quad a = 0.44\,\text{m},\quad b = 0.64\,\text{m},\quad b_0 = 0.68\,\text{m}. \tag{83}$$

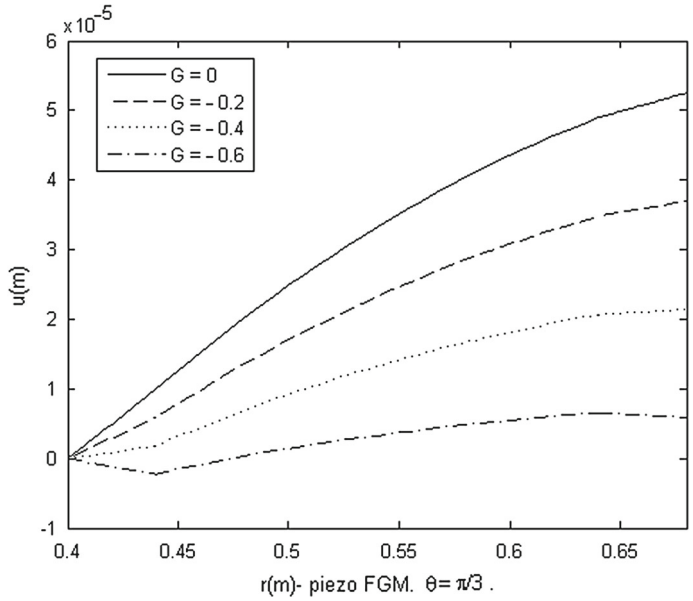

Fig. 14 Radial displacement distribution in the piezo-FGM hollow sphere with various G, where $m = 1$ at $\theta = \pi/3$

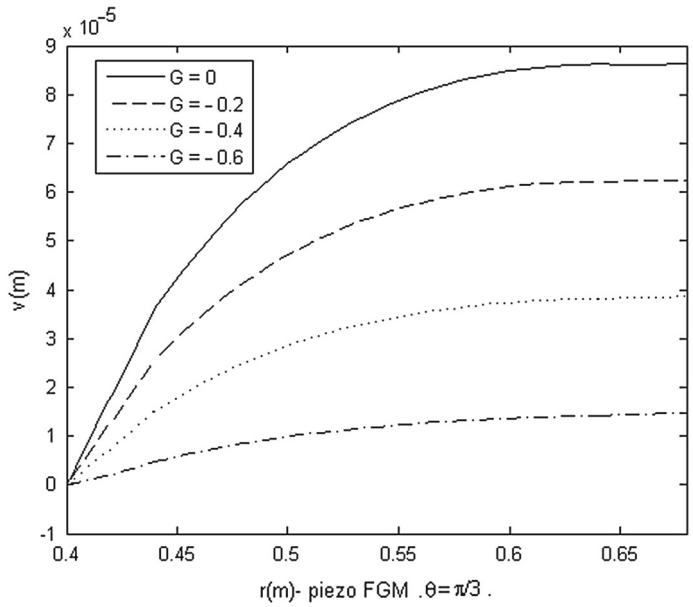

Fig. 15 Circumferential displacement distribution in the piezo-FGM hollow sphere with various G, where $m = 1$ at $\theta = \pi/3$

The following are material constants considered for piezoelectric layers (PZT-4):

$$C_{11} = 139\ \text{GPa}, \quad C_{12} = 78\,\text{GPa}, \quad C_{13} = 74.3\ \text{GPa}, \quad C_{33} = 115\,\text{GPa}, \quad C_{44} = 25.6\,\text{GPa},$$
$$\alpha = 2.4 \times 10^{-6}\left(\text{K}^{-1}\right), \quad k_p = 1.5(\text{Wm}^{-1}\,\text{K}^{-1}),$$
$$e_{21} = -5.2\left(\text{Cm}^{-2}\right), \quad e_{22} = 15.1\left(\text{Cm}^{-2}\right), \quad e_{25} = 12.7\left(\text{Cm}^{-2}\right),$$
$$g_{21} = -2.94 \times 10^{-6}\left(\text{Cm}^{-2}\,\text{K}^{-1}\right), \quad g_{22} = -2.94 \times 10^{-6}\left(\text{Cm}^{-2}\,\text{K}^{-1}\right),$$
$$\varepsilon_{11} = 64.64 \times 10^{-10}\left(\text{Fm}^{-1}\right), \quad \varepsilon_{22} = 56.22 \times 10^{-10}\left(\text{Fm}^{-1}\right).$$

And the material properties of the FGM layer are

$$E_0 = 200\,\text{GPa}, \quad \alpha_0 = 1.2 \times 10^{-6}\,\text{K}^{-1}, \quad \nu = 0.3, \quad k_m = 2\text{Wm}^{-1}\,\text{K}^{-1}. \tag{84}$$

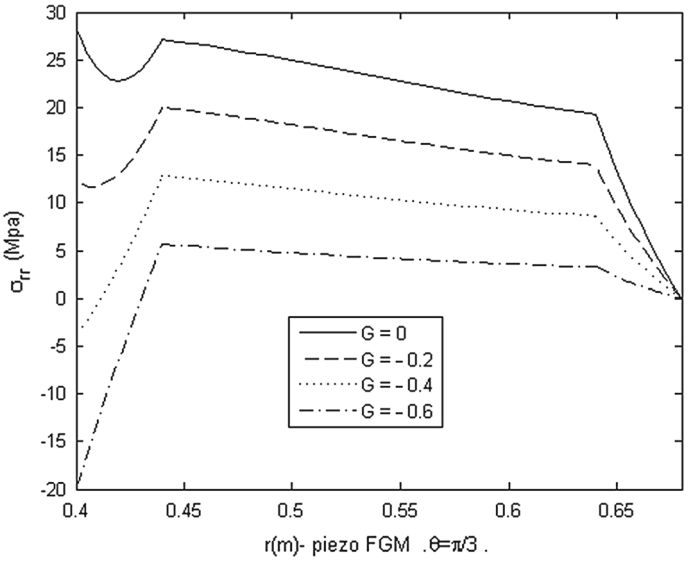

Fig. 16 Radial stress distribution in the piezo-FGM hollow sphere with various G, where $m = 1$ at $\theta = \pi/3$

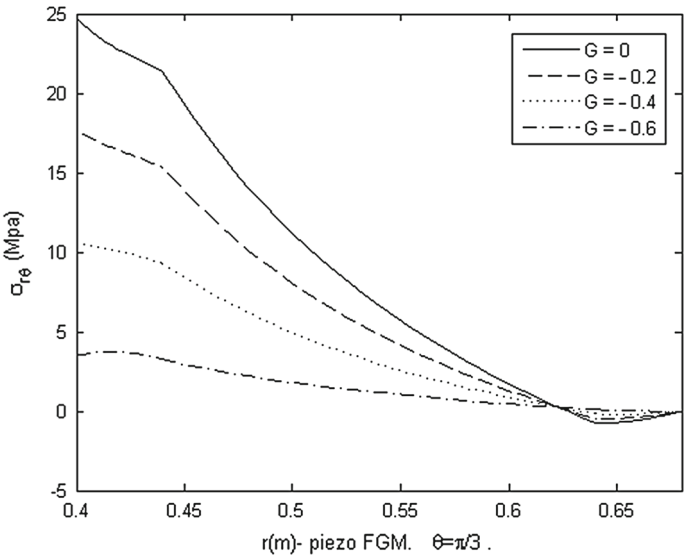

Fig. 17 Shear stress distribution in the piezo-FGM hollow sphere with various G, where $m = 1$ at $\theta = \pi/3$

The power of material properties is considered as identical, $m_1 = m_2 = m_3 = m$.

Example 1. In this example, the inside surface of the inner layer (sensor) is assumed to be heated and cooled by a temperature distribution given by $T^s(a_0, \theta) = 30P_1(\cos\theta)$. The outside surface of the outer layer (actuator) is considered in zero temperature. Traction-free conditions are assumed at the outside surface ($r = b_0$), and the inside surface ($r = a_0$) is assumed to be fixed in r and θ directions. The thermal, mechanical, and electrical boundary conditions are as follows:

$$T^s(a_0, \theta) = 30P_1(\cos\theta), \quad T^a(b_0, \theta) = 0, \tag{85}$$

$$u^s(a_0, \theta) = 0, \quad v^s(a_0, \theta) = 0, \tag{86a}$$
$$\sigma^a_{rr}(b_0, \theta) = 0, \quad \sigma^a_{r\theta}(b_0, \theta) = 0, \tag{86b}$$

$$\varphi^s(a, \theta) = 0, \quad D^s_{rr}(a_0, \theta) = 0, \tag{87a}$$
$$\varphi^a(b, \theta) = 0, \quad \varphi^a(b_0, \theta) = 0. \tag{87b}$$

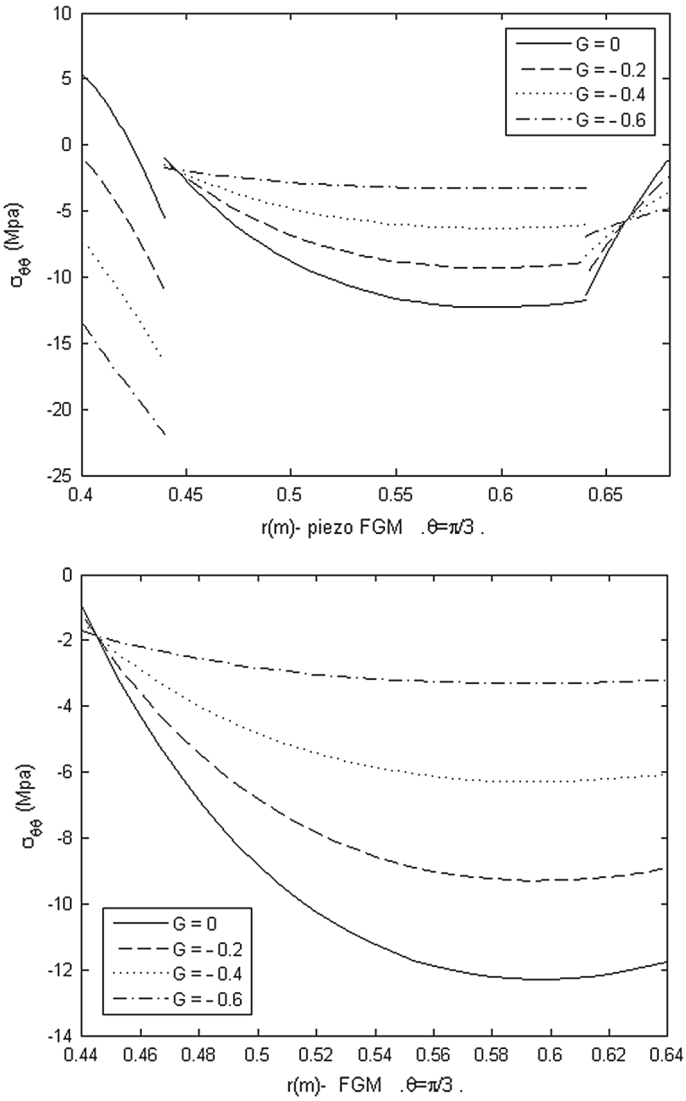

Fig. 18 a Circumferential stress distribution in the piezo-FGM hollow sphere with various G, where $m = 1$ at $\theta = \pi/3$. **b** Circumferential stress distribution in the FGM layer with various G, where $m = 1$ at $\theta = \pi/3$ (host layer)

As determined from Eq. (87b) in this example, the input control voltage to the actuator layer is zero, which means there is no active control over the structure. The example shows the significant influence of the grading index of material properties "m" on the mechanical and electrical response of the piezo-FGM structure.

Figure 2 is the temperature distribution along the radius at $\theta = \pi/3$ for different power law indices. The temperature distribution follows the given boundary conditions at the inside and outside surfaces. For different values of m, radial and circumferential displacement, radial stress, shear stress, and circumferential stress along the radial direction at $\theta = \pi/3$ are plotted in Figs. 3, 4, 5, 6, and 7, respectively. From Figs. 3 and 4, one can see that the radial and circumferential displacement decreases as the graded index m increases in the same radial point at $\theta = \pi/3$, respectively. It can easily be seen from Figs. 5 and 6 that the radial and shear stress at the external boundaries which satisfy the given mechanical boundary conditions decreases as the graded index m increases along the radial direction at $\theta = \pi/3$. The distribution of circumferential stress along the radial direction at $\theta = \pi/3$ is shown in Fig. 7, and the magnitude of the circumferential stress is decreased as the power index m is increased.

Figures 8 and 9 show radial electrical displacement distributions along the radius at $\theta = \pi/3$ in the piezo layers with various m. It can easily be seen from Fig. 8 that radial electrical displacement decreases as the

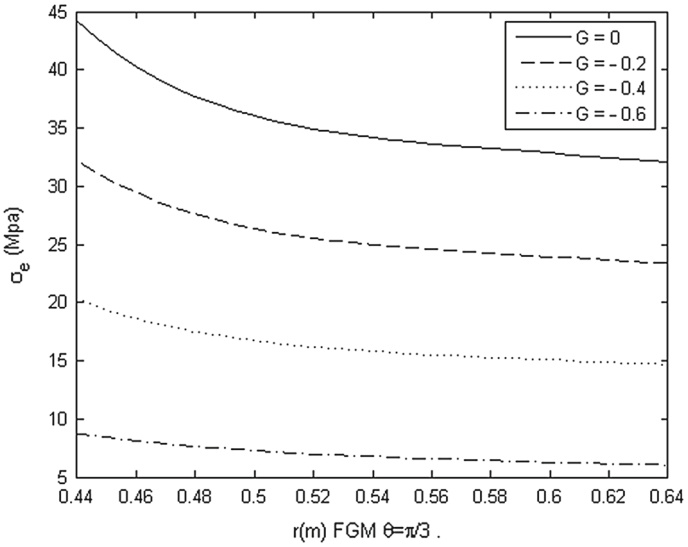

Fig. 19 Effective stress distribution in the FGM layer with various G, where $m = 1$ at $\theta = \pi/3$ (host layer)

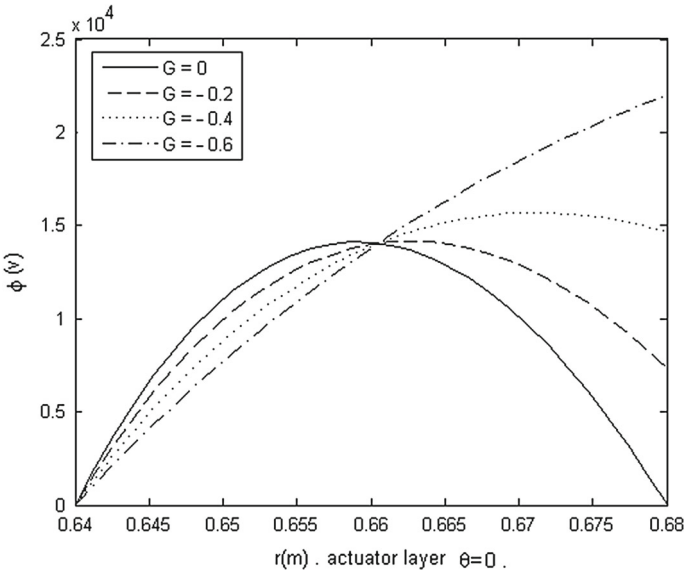

Fig. 20 Electric potential distribution in the actuator layer with various G, where $m = 1$ at $\theta = 0$

graded index m increases at the same radial point in the sensor layer. The distribution of electric potential in the sensor and actuator layers along the radius at $\theta = 0$ is shown in Figs. 10 and 11, respectively. It can easily be seen from Figs. 10 and 11 that electric potential satisfies the prescribed electrical boundary conditions. Here, the magnitude of the electric potential is decreased as the power index m is increased in sensor and actuator layers. The plots of circumferential electrical displacement distributions along the radius at $\theta = \pi/3$ in the piezo layers with various m are shown in Figs. 12 and 13. It can easily be seen from Fig. 12 that the circumferential electrical displacements decrease as the power index m is increases at the same radial point in sensor layer.

Example 2. In this example, which shows the control aspect of the article, the electrical boundary conditions of the smart FGM structure (Fig. 1), in which the inner and outer piezoelectric layers serve, respectively, as the sensor and actuator, which are linked by a constant gain control algorithm, are, respectively, taken as

$$\varphi^s(a,\theta) = 0, \qquad D^s_{rr}(a_0,\theta) = 0, \tag{88a}$$

$$\varphi^a(b,\theta) = 0, \qquad \varphi^a(b_0,\theta) = V^a P_1(\cos\theta) = G\, V^s P_1(\cos\theta). \tag{88b}$$

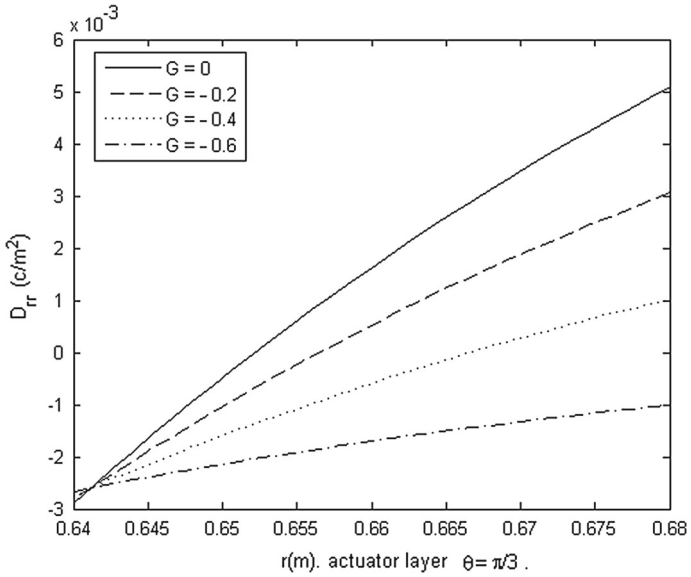

Fig. 21 Radial electrical displacement in the actuator layer with various G, where $m = 1$ at $\theta = \pi/3$

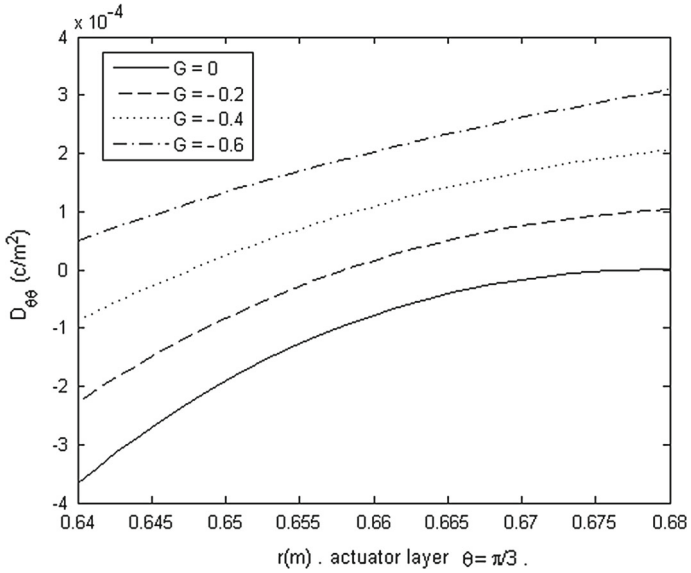

Fig. 22 Circumferential electrical displacement in the actuator layer with various G, where $m = 1$ at $\theta = \pi/3$

In this example, the mechanical and thermal boundary conditions are according to the relations (85)–(86), as in Example 1. In this example, when the Piezo-FGM structure suffers thermal strain, the piezoelectric sensor generates an output voltage, and this voltage can be amplified and feedback to the actuator. The piezoelectric actuator converts the input voltage into a strain/displacement actuation and transmits this actuation to the main structure (FGM layer) in order to modify its mechanical state. Thus, in this example, the effect of the control voltage on the mechanical response of structures will be presented. Here, the graded index is $m = 1$, and it is noteworthy that Fig. 10 illustrates the electric potential distribution in the sensor layer (while $m = 1$). Also, Fig. 2 is the temperature distribution along the radius (while $m = 1$).

Figures 14, 15, 16, 17, and 18 show the distributions of radial and circumferential displacement, radial stress, shear stress, and circumferential stress along the radial direction at $\theta = \pi/3$ in the piezo-FGM hollow sphere with different values of G(feedback gain), respectively. Here, from Figs. 14 and 15, one can see that the radial and circumferential displacement decreases considerably with the increase in the negative feedback gain G (from $G = 0$ to $G = -0.6$) at the same radial point, respectively. It can easily be seen from Figs. 16 and 17 that

the radial and shear stress at the external boundaries which satisfy the given mechanical boundary conditions decreases considerably with the increase in the negative feedback gain in Figs. 16 and 17, respectively. The distribution of circumferential stress along the radial direction at $\theta = \pi/3$ is shown in Fig. 18, and the magnitude of the circumferential stress is decreased as there is increase in the negative feedback gain, noticeably.

The effective stress in the FGM layer is significantly reduced.

It is noteworthy that the effective stress in the FGM layer is considered to be in accordance with the following formula:

$$\sigma_e^F = \sqrt{\left(\sigma_{rr}^F - \sigma_{\theta\theta}^F\right)^2 + \left(\sigma_{\theta\theta}^F - \sigma_{\varphi\varphi}^F\right)^2 + \left(\sigma_{rr}^F - \sigma_{\varphi\varphi}^F\right)^2 + 6\left(\sigma_{r\theta}^F\right)^2}/\sqrt{2}. \tag{89}$$

From Figs. 14, 15, 16, 17, 18, and 19, it is clear that with the increase in the negative feedback gain parameter G, and in fact, with the increase in the input control voltage to the actuator layer, the deformation and thermal stress in the FGM layer are controlled, i.e., considerably reduced.

The distribution of electric potential in the actuator layer along the radius at $\theta = 0$ with different values of G is shown in Fig. 20 (while $m = 1$). It can easily be seen from Fig. 20 that electric potential satisfies the prescribed electrical boundary conditions.

Figure 21 is the plot of radial electrical displacement in the actuator layer. It can easily be seen that the radial electrical displacement decreases from outer surface to inner surface of the actuator layer as the negative feedback gain increases at the same radial point. The plot of circumferential electrical displacement distributions along the radius at $\theta = \pi/3$ in actuator layer with various G is shown in Fig. 22 (while $m = 1$). From Fig. 22, one can see that, with the increase in the negative feedback gain, the magnitude of the circumferential electrical displacement decreases.

6 Conclusions

In this article, an analytical study of piezothermoelastic behavior and controls of an FGM hollow sphere with an integrated piezoelectric sensor and actuator under non-axisymmetric thermal loads is presented. A feedback control algorithm coupling the direct and inverse piezoelectric effects is applied via a closed-loop system to provide feedback control of the piezothermoelastic response of the multilayered hollow sphere. Thermal, mechanical, and electrical boundary conditions are assumed to be the functions of the variables r and θ. A power law model is considered for the variations in the FGM profiles. Direct method of solution based on the power series and Legendre functions is used to obtain the solution of governing differential equations. Numerical examples are given and discussed to show the significant influence of the grading index of material properties and negative feedback gain on the mechanical–electrical responses. The conclusions are:

(i) Numerical results in Example 1 show that the graded index m has a great effect on the piezothermoelectric behavior of a smart FGM hollow sphere, and adopting a certain value of the m can optimize the responses. It is possible for engineers to design piezo-FGM spherical structures that can meet some special requirements.

(ii) Through the results in Example 2, it can be concluded that it is possible to an active control of stress/displacement of the FGM hollow sphere by applying a suitable negative feedback gain. This will be of particular importance in modern engineering design.

Appendix A

Consider the Legendre differential equation [34] as

$$\left(1 - x^2\right) y''(x) - 2xy'(x) + n(n+1)\, y(x) = 0,$$

where x and y are independent and dependent variables, respectively. The solution of the foregoing differential equation is

$$y(x) = P_n(x),$$

where $P_n(x)$ is a Legendre polynomial and may be written as

$$P_n(x) = \frac{1}{2^n n!} \frac{\mathrm{d}^n}{\mathrm{d}x^n} (x^2 - 1)^n.$$

Utilizing Eqs. (46)–(48), the following relations may be derived

$$
\begin{aligned}
&(x^2-1)P_n'(x) = nxP_n(x) - nP_{n-1}(x),\\
&2(x^2-1)P_n''(x) + xP_n'(x) = nxP_n'(x) + nP_n(x) - nP_{n-1}(x),\\
&xP_n'(x) - P_{n-1}(x) = nP_n(x),\\
&(x^2-1)P_n''(x) + 2xP_n'(x) = \left(n+n^2\right)P_n(x).
\end{aligned}
$$

Appendix B

$$
\begin{aligned}
d_1^{a,s} &= \beta_{n1}^{a,s}\left(\beta_{n1}^{a,s}+1\right) + 2\left(\beta_{n1}^{a,s}+1\right) + \left(\frac{-n(n+1)c_{44} + 2c_{13} - 2(c_{11}+c_{12})}{c_{33}}\right),\\
d_2^{a,s} &= \beta_{n2}^{a,s}\left(\beta_{n2}^{a,s}+1\right) + 2\left(\beta_{n2}^{a,s}+1\right) + \left(\frac{-n(n+1)c_{44} + 2c_{13} - 2(c_{11}+c_{12})}{c_{33}}\right),\\
d_3^{a,s} &= \left(\frac{n(n+1)(c_{44}+c_{13})}{c_{33}}\right)\left(\beta_{n1}^{a,s}+1\right) + \left(\frac{n(n+1)(c_{13}-(c_{44}+c_{11}+c_{12}))}{c_{33}}\right),\\
d_4^{a,s} &= \left(\frac{n(n+1)(c_{44}+c_{13})}{c_{33}}\right)\left(\beta_{n2}^{a,s}+1\right) + \left(\frac{n(n+1)(c_{13}-(c_{44}+c_{11}+c_{12}))}{c_{33}}\right),\\
d_5^{a,s} &= \left(\frac{e_{22}}{c_{33}}\right)\beta_{n1}^{a,s}\left(\beta_{n1}^{a,s}+1\right) + \left(\frac{2(e_{22}-e_{21})}{c_{33}}\right)\left(\beta_{n1}^{a,s}+1\right) - n(n+1)\frac{e_{25}}{c_{33}},\\
d_6^{a,s} &= \left(\frac{e_{22}}{c_{33}}\right)\beta_{n2}^{a,s}\left(\beta_{n2}^{a,s}+1\right) + \left(\frac{2(e_{22}-e_{21})}{c_{33}}\right)\left(\beta_{n2}^{a,s}+1\right) - n(n+1)\frac{e_{25}}{c_{33}},\\
d_7^{a,s} &= \frac{z_r}{c_{33}}\left(1-f+\beta_{n1}^{a,s}\right)A_{n1}^{a,s},\\
d_8^{a,s} &= \frac{z_r}{c_{33}}\left(1-f+\beta_{n2}^{a,s}\right)A_{n2}^{a,s},\\
d_9^{a,s} &= \beta_{n1}^{a,s}\left(\beta_{n1}^{a,s}+1\right) + 2\left(\beta_{n1}^{a,s}+1\right) - \left(2+n(n+1)\frac{c_{11}}{c_{44}} + \frac{c_{12}}{c_{44}}\right),\\
d_{10}^{a,s} &= \beta_{n2}^{a,s}\left(\beta_{n2}^{a,s}+1\right) + 2\left(\beta_{n2}^{a,s}+1\right) - \left(2+n(n+1)\frac{c_{11}}{c_{44}} + \frac{c_{12}}{c_{44}}\right),\\
d_{11}^{a,s} &= -\left(1+\frac{c_{13}}{c_{44}}\right)\left(\beta_{n1}^{a,s}+1\right) - \left(2+\frac{c_{11}+c_{12}}{c_{44}}\right),\\
d_{12}^{a,s} &= -\left(1+\frac{c_{13}}{c_{44}}\right)\left(\beta_{n2}^{a,s}+1\right) - \left(2+\frac{c_{11}+c_{12}}{c_{44}}\right),\\
d_{13}^{a,s} &= -2\frac{e_{25}}{c_{44}} - \left(\frac{e_{25}+e_{21}}{c_{44}}\right)\left(\beta_{n1}^{a,s}+1\right),\\
d_{14}^{a,s} &= -2\frac{e_{25}}{c_{44}} - \left(\frac{e_{25}+e_{21}}{c_{44}}\right)\left(\beta_{n2}^{a,s}+1\right),\\
d_{15}^{a,s} &= \frac{-fz_r}{c_{44}}A_{n1}^{a,s}, \quad d_{16}^{a,s} = \frac{-fz_r}{c_{44}}A_{n2}^{a,s},\\
d_{17}^{a,s} &= \beta_{n1}^{a,s}\left(\beta_{n1}^{a,s}+1\right) + \left(2+\frac{2e_{21}}{e_{22}}\right)\left(\beta_{n1}^{a,s}+1\right) + \left(\frac{e_{21}}{e_{22}} - n(n+1)\frac{e_{25}}{e_{22}}\right),\\
d_{18}^{a,s} &= \beta_{n2}^{a,s}\left(\beta_{n2}^{a,s}+1\right) + \left(2+\frac{2e_{21}}{e_{22}}\right)\left(\beta_{n2}^{a,s}+1\right) + \left(\frac{e_{21}}{e_{22}} - n(n+1)\frac{e_{25}}{e_{22}}\right),\\
d_{19}^{a,s} &= n(n+1)\left(\frac{e_{21}+e_{25}}{e_{22}}\right)\left(\beta_{n1}^{a,s}+1\right) - n(n+1)\left(\frac{e_{21}}{e_{22}} - \frac{e_{25}}{e_{22}}\right),
\end{aligned}
$$

$$
\begin{aligned}
d_{20}^{a,s} &= n\,(n+1)\left(\frac{e_{21}+e_{25}}{e_{22}}\right)\left(\beta_{n2}^{a,s}+1\right)-n\,(n+1)\left(\frac{e_{21}}{e_{22}}-\frac{e_{25}}{e_{22}}\right),\\
d_{21}^{a,s} &= -\left(\frac{\varepsilon_{22}}{e_{22}}\right)\beta_{n1}^{a,s}\left(\beta_{n1}^{a,s}+1\right)-2\left(\frac{\varepsilon_{22}}{e_{22}}\right)\left(\beta_{n1}^{a,s}+1\right)+n\,(n+1)\left(\frac{\varepsilon_{11}}{e_{22}}\right),\\
d_{22}^{a,s} &= -\left(\frac{\varepsilon_{22}}{e_{22}}\right)\beta_{n2}^{a,s}\left(\beta_{n2}^{a,s}+1\right)-2\left(\frac{\varepsilon_{22}}{e_{22}}\right)\left(\beta_{n2}^{a,s}+1\right)+n\,(n+1)\left(\frac{\varepsilon_{11}}{e_{22}}\right),\\
d_{23}^{a,s} &= -\left(\frac{g_{22}}{e_{22}}\right)(2+sn\,(n+1)+\beta_{n1}^{a,s})A_{n1}^{a,s},\\
d_{24}^{a,s} &= -\left(\frac{g_{22}}{e_{22}}\right)(2+sn\,(n+1)+\beta_{n2}^{a,s})A_{n2}^{a,s}.
\end{aligned}
$$

Appendix C

$$
\begin{aligned}
d_1^F &= \left(\beta_{n1}^F+m_2+1\right)\left(\beta_{n1}^F+m_2\right)+(m_1+2)\left(\beta_{n1}^F+m_2+1\right)+\frac{2\nu m_1}{1-\nu}-n\,(n+1)\,\frac{1-2\nu}{1-\nu}-2,\\
d_2^F &= \left(\beta_{n2}^F+m_2+1\right)\left(\beta_{n2}^F+m_2\right)+(m_1+2)\left(\beta_{n2}^F+m_2+1\right)+\frac{2\nu m_1}{1-\nu}-n\,(n+1)\,\frac{1-2\nu}{1-\nu}-2,\\
d_3^F &= \frac{n\,(n+1)}{2-2\nu}\left(\left(\beta_{n1}^F+m_2+1\right)+2\nu m_1-3+4\nu\right),\\
d_4^F &= \frac{n\,(n+1)}{2-2\nu}\left(\left(\beta_{n2}^F+m_2+1\right)+2\nu m_1-3+4\nu\right),\\
d_5^F &= \frac{\alpha_0(1+\nu)}{1-\nu}\left(\beta_{n1}^F+m_1+m_2\right)A_{n1}^F,\\
d_6^F &= \frac{\alpha_0(1+\nu)}{1-\nu}\left(\beta_{n2}^F+m_1+m_2\right)A_{n2}^F,\\
d_7^F &= \left(\beta_{n1}^F+m_2\right)\left(\beta_{n1}^F+m_1+m_2+2\right)-m_1-n\,(n+1)\,\frac{2-2\nu}{1-2\nu},\\
d_8^F &= \left(\beta_{n2}^F+m_2\right)\left(\beta_{n2}^F+m_1+m_2+2\right)-m_1-n\,(n+1)\,\frac{2-2\nu}{1-2\nu},\\
d_9^F &= -\frac{1}{1-2\nu}\left(\beta_{n1}^F+(1-2\nu)\,m_1+m_2+5-4\nu\right),\\
d_{10}^F &= -\frac{1}{1-2\nu}\left(\beta_{n2}^F+(1-2\nu)\,m_1+m_2+5-4\nu\right),\\
d_{11}^F &= -\frac{\alpha_0(1+\nu)}{1-2\nu}A_{n1}^F,\\
d_{12}^F &= -\frac{\alpha_0(1+\nu)}{1-2\nu}A_{n2}^F.
\end{aligned}
$$

References

1. Ding, H.J., Chen, W.Q.: Three Dimensional Problems of Piezoelasticity. Nova Science Publishers, New York (2001)
2. Ootao, Y., Tanigawa, Y.: Control of transient thermoelastic displacement of a two-layered composite plate constructed of isotropic elastic and piezoelectric layers due to nonuniform heating. Arch. Appl. Mech. **71**, 207–220 (2001)
3. Ashida, F., Tauchert, T.R.: A general plane-stress solution in cylindrical coordinates for a piezothermoelastic plate. Int. J. Solids Struct. **38**, 4969–4985 (2001)
4. Qin, Q.H., Mai, Y.W.: Thermoelectroelastic Green's function and its application for bimaterial of piezoelectric materials. Arch. Appl. Mech. **68**, 433–444 (1998)
5. Shul'ga, N.A.: Radial electro-elastic vibrations of a hollow piezoceramic sphere. J. Appl. Mech. **22**, 731–734 (1990)

6. Ding, H.J., Wang, H.M., Chen, W.Q.: Analytical solution for a non-homogeneous isotropic piezoelectric hollow sphere. Arch. Appl. Mech. **73**, 49–62 (2003)
7. Chen, W.Q., Shioya, T.: Piezothermoelastic behavior of a pyroelectric spherical shell. J. Therm. Stress **24**, 105–120 (2001)
8. Chen, W.Q., Lu, Y., Ye, G.R. et al.: 3D electroelastic fields in a functionally graded piezoceramic hollow sphere under mechanical and electric loadings. Arch. Appl. Mech. **72**, 39–51 (2002)
9. Dai, H.L., Wang, X.: Thermo-electro-elastic transient responses in piezoelectric hollow structures. Int. J. Solids Struct. **42**, 1151–1171 (2005)
10. Ootao, Y., Tanigawa, Y.: Transient piezothermoelastic analysis for a functionally graded thermopiezo electric hollow sphere. Compos. Struct. **81**(4), 540–549 (2007)
11. Wang, H.M., Ding, H.J., Chen, Y.M.: Transient responses of a multilayered spherically isotropic piezoelectric hollow sphere. Arch. Appl. Mech. **74**, 581–599 (2005)
12. Wang, H.M., Xu, Z.X.: Effect of material inhomogeneity on electromechanical behaviors of functionally graded piezoelectric spherical structures. Comput. Mater. Sci. **48**, 440–445 (2010)
13. Chen, W.Q., Ding, H.J., Xu, R.Q.: Three-dimensional free vibration analysis of a fluid-filled piezoceramic hollow sphere. Comput. Struct. **79**, 653–663 (2001)
14. Chen, W.Q., Ding, H.J., Xu, R.Q.: Three dimensional static analysis of multi-layered piezo electric hollow sphere via the state space method. Int. J. Solids Struct. **38**, 4921–4936 (2001)
15. Liu, C.B., Bian, Z.G., Chen, W.Q., Lü, C.F.: Three-dimensional pyroelectric analysis of a functionally graded piezoelectric hollow sphere. J. Therm. Stress. **35**, 499–516 (2012)
16. Jabbari, M., Karampour, S., Eslami, M.R.: Steady state thermal and mechanical stresses of a poro-piezo-FGM hollow sphere. Meccanica **48**, 699–719 (2013)
17. Eslami, M.R., Babaei, M.H., Poultangari, R.: Thermal and mechanical stresses in a functionally graded thick sphere. Int. J. Press. Vessel Pip. **82**(7), 452–457 (2005)
18. Obata, Y., Noda, N.: Steady thermal stresses in a hollow circular cylinder and a hollow sphere of a functionally gradient material. J. Therm. Stress. **17**(3), 471–487 (1994)
19. Jabbari, M., Sohrabpour, S., Eslami, M.R.: Mechanical and thermal stresses in functionally graded hollow cylinder due to radially symmetric loads. Int. J. Press. Vessel Pip. **79**, 493–497 (2002)
20. Jabbari, M., Sohrabpour, S., Eslami, M.R.: General solution for mechanical and thermal stresses in a functionally graded hollow cylinder due to nonaxisymmetric steady-state loads. ASME J. Appl. Mech. **70**, 111–118 (2003)
21. Poultangari, R., Jabbari, M., Eslami, M.R.: Functionally graded hollow spheres under non-axisymmetric thermo-mechanical loads. Int. J. Press. Vessels Pip. **85**(5), 295–305 (2008)
22. Ootao, Y., Tanigawa, Y.: Three-dimensional transient piezothermoelasticity in functionally graded rectangular plate bonded to a piezoelectric plate. Int. J. Solids Struct. **37**, 4377–4401 (2000)
23. Reddy, J.N., Cheng, Z.Q.: Three-dimensional solutions of smart functionally graded plates. J. Appl. Mech. **68**, 234–241 (2001)
24. Wang, B.L., Noda, N.: Design of smart functionally graded thermo-piezoelectric composite structure. Smart Mater. Struct. **10**, 189–193 (2001)
25. Huang, X.L., Shen, H.S.: Vibration and dynamic response of functionally graded plates with piezoelectric actuators in thermal environments. J. Sound Vib. **289**, 25–53 (2006)
26. Reddy, J.N.: Mechanics of Laminated Composite Plates and Shells, Conservative. 2nd edn. CRC Press, New York (2004)
27. Liew, K.M., He, X.Q., Ng, T.Y. et al.: Active control of FGM plates subjected to a temperature gradient: Modelling via finite element method based on FSDT. Int. J. Numer. Methods Eng. **52**, 1253–1271 (2001)
28. Liew, K.M., He, X.Q., Ng, T.Y. et al.: Finite element piezothermoelasticity analysis and the active control of FGM plates with integrated piezoelectric sensors and actuators. Comput. Mech. **31**, 350–358 (2003)
29. Liew, K.M., He, X.Q., Ng, T.Y. et al.: Active control of FGM shells subjected to a temperature gradient via piezoelectric sensor/actuator patches. Int. J. Numer. Methods Eng. **55**, 653–668 (2002)
30. Sabzikar Boroujerdy, M., Eslami, M.R.: Nonlinear axisymmetric thermomechanical response of piezo-FGM shallow spherical shells. Arch. Appl. Mech. **83**, 1681–1693 (2013)
31. Ahmad, G., Manouchehr, S., Saeed, F.: Deflection control of functionally graded material beams with bonded piezoelectric sensors and actuators. Mater. Sci. Eng. A **498**, 110–114 (2008)
32. Xiao, L.H., Shen, H.S.: Vibration and dynamic response of functionally graded plates with piezoelectric actuators in thermal environments. J. Sound Vib. **289**, 25–53 (2006)
33. He, X.Q., Hg, Y.Y., Sivashanker, S.: Active control of FGM plates with integrated piezoelectric sensors and actuators. Int. J. Solids Struct. **38**, 1641–1655 (2001)
34. Korn, G.A., Korn, T.M.: Mathematical Handbook for Scientists and Engineers. McGraw-Hill, New York (1968)